

João Afonso Azevedo Pereira da Silva

# Characterization of novel $\beta$ I integrin interactors involved in the regulation $\beta$ I integrin trafficking

Tese de mestrado em Investigação Biomédica, ramo de Bioquímica e Medicina Molecular,  
sob orientação científica do Doutor Ralph Thomas Böttcher  
apresentada à Faculdade de Medicina da Universidade de Coimbra

Junho de 2016



UNIVERSIDADE DE COIMBRA

# **Characterization of novel $\beta 1$ integrin interactors involved in the regulation $\beta 1$ integrin trafficking**

João Afonso Azevedo Pereira da Silva

Dissertação apresentada à Faculdade de Medicina da Universidade de Coimbra para cumprimento dos requisitos necessários à obtenção do grau de Mestre em Investigação Biomédica. Trabalho realizado no Departamento de Medicina Molecular do Instituto Max Planck de Bioquímica em Munique, sob a orientação científica do Dr. Ralph Thomas Böttcher

Universidade de Coimbra

2016



(On the cover: WDR11 co-localizing with the *trans*-Golgi network in a HeLa cell.  
Image was acquired using confocal microscopy)



*“There's real poetry in the real world. Science is the poetry of reality”*

Richard Dawkins



# Agradecimentos

Ao Ralph Böttcher por me ter proporcionado a oportunidade de desenvolver este projecto de tese como membro do seu grupo de investigação, e na qualidade de supervisor, agradecer por toda a experiência e conhecimento científico transmitida ao longo deste ano e por promover em mim um espírito crítico, de clareza e de organização em todo o processo de “fazer ciência”. Quero também deixar um sincero agradecimento ao Professor Reinhard Fässler por me ter dado a oportunidade de trabalhar no Departamento de Medicina Molecular e no seu laboratório, assim como de poder fazer parte do Instituto Max Planck de Bioquímica, sem o qual nada disto teria sido possível.

Um agradecimento muito especial à adorável Valeria Samarelli. Obrigado por toda a abertura, disponibilide, simpatia e amabilidade com que desde o primeiro dia me recebeste, e com que sempre me ouviste e prontamente esclareceste todas as minhas dúvidas e perguntas, mesmo as às vezes um pouco menos pertinentes. Por todas as pequenas coisas que fizeste e que me ajudaram fazer passar este primeiro ano fora de casa e longe meu país de uma forma mais positiva e optimista. Ao Tilman Ziegler por todo o input, paciência e conhecimento que me transmitiu ao longo do ano e por todos os momentos mais relaxados e divertidos dentro e fora do lab. Agradecer também à Mischa, à Sarah Schölze e ao Tom por toda a ajuda e orientação que sempre me deram no lab. Não podia faltar o agradecimento à Marina, à Georgina, à Maria e à Lidia por toda a diversão, ajuda e motivação para cada dia no laboratório. Aos meus colegas portugueses, um muito obrigado à Ana Keating pela ajuda com a tese, pelos copos e pelas pausas, ao Pedro Melo, e em especial também à Irene Ferreira por toda a paciência, disponibilidade e abertura para me ajudar de forma indispensável a preparar e guiar me para o meu futuro e por mostrar que existe mais desafios fora do lab. E claro, agradecer a todos os outros colegas do Dept. de Medicina Molecular, em particular do ao 1º andar por serem meus colegas de trabalho e nunca me negarem auxílio sempre que precisei.



Ao Manuel Conde pela amizade criada entre 2 portugueses acabados de chegar a Munique, pelas viagens, jantares, noites & co. e tudo o resto. E que no fundo foram essenciais para que o ano de Erasmus fosse mais descomprimido e bem passado.

Aos meus colegas do MIB 2014, que apesar de a distancia nos ter separado este ano, tiveram um papel preponderante no ano que viria a dar a este no qual espero, com esta tese, terminar mais outro ciclo de estudos. Por todos os convívios, jantares, saídas, trabalhos e ajuda partilhados no primeiro ano.

Por fim, mas de certeza não menos importante, agradecimento à minha família, em especial aos meus pais, por todos os enormes sacrifícios dia após dia que permitiram estar onde estou hoje e chegar aonde cheguei. Pela a constante preocupação e dedicação em proporcionar-me uma vida com o melhor que têm para dar. Por me ajudarem nos momentos mais difíceis não só neste ano de distância, mas ao longo de toda a minha vida e fazerem de mim a pessoa que sou hoje. Um eterno obrigado!

# Acknowledgements

First and foremost, I want to thank Ralph Böttcher for providing this opportunity to develop this thesis project as a member of his investigation group and as a supervisor, thank all the experience and scientific knowledge transmitted during this year and for promoting in me a more critical thinking and organization attitude in all the process of “making science”. I also want to express my sincere gratitude to Professor Reinhard Fässler for allowing me the chance to work in the Molecular Medicine Dept. and his lab, as well as being able to be part of the Max Planck Institute for Biochemistry, without whom none of this would have been possible.

A very much special thank you to the lovely Valeria Samarelli. Thank you for all the openness, availability, kindness and heartfelt sympathy with which you received me from the first day, and how with all of that you always readily listened to my questions and doubts, sometimes even when they were less convenient and thought through. For all the things you made that helped me carry on through this first year out of home and far away from my country in a more optimistic and positive way. To Tilman Ziegler for all the input, patience and knowledge he provided me during this year, and for all the funny and relaxed moments we enjoyed in and outside of the lab. Also want to thank Mischa, Sara Schölze and Tom for all the help and guidance always given in the lab. I could not forget to thank Marina, Georgina, Maria and Lidia for all the amusement, help and motivation for each day that went through in the lab.

To my Portuguese colleagues, a big thank you to Ana Keating for all the help with the thesis, the drinks and the lab breaks, to Pedro Melo, and specially to Irene Ferreira for all the patience, availability and readiness in helping me, for all the guidance and support in preparing my future steps and for showing me there are more challenges besides the ones in the lab. And of course, thank all my Molecular Medicine Dept. colleagues, in particular the 1<sup>st</sup> floor por being my work colleagues and always help me when I needed.

Many thanks to Manuel Conde for the friendship created between 2 Portuguese just arrived in München, for the trips, dinners, nights out & co and everything else. Which in the end were indispensable for this Erasmus year to run smoothly and chilled out.

To my MIB 2014 colleagues, despite distance separated us this year, still had a remarkable role in the year before this one, in which with thesis, I hope to finish another degree. Thank you for all the get togethers, dinners, night outs, works and help shared in that first year.

Last, but definitely not the least, thank my family, specially my parents, for all the sacrifices day after day that allowed me to be where I am today and accomplish what I've accomplished. For the constant concern and dedication in providing me a life with the best they have to give. For helping me in all the hard moments not only in this year apart, but through all my entire life and for making me the person I am today. An everlasting Thank You!

# Table of Contents

List of figures.....	XIII
Abstract.....	XVII
Resumo.....	XIX
<u>INTRODUCTION</u> .....	1
1. Integrin Overview.....	3
1.1. Integrin Structure .....	3
1.1.1. $\alpha\beta$ Subunits.....	4
1.1.2. Intracellular Domains - Cytoplasmic tails .....	5
1.1.3. Transmembrane Domains.....	5
1.1.4. Extracellular Domains .....	5
1.2. Integrin Signaling and Function .....	5
1.3. $\alpha5\beta1$ Integrin and Cell Migration.....	6
2. Integrin Trafficking .....	7
2.1. Canonical Trafficking .....	7
2.1.1. Clathrin-dependent endocytosis of integrins.....	7
2.1.2. Clathrin-independent endocytosis of integrins.....	8
2.1.3. Recycling: Short-loop pathway .....	8
2.1.4. Recycling: Long-loop pathway .....	9
3. Golgi-mediated Trafficking.....	9
3.1. Retrograde Trafficking and the <i>trans</i> -Golgi network .....	10
3.1.1. Early endosome-to-TGN pathway.....	11
3.1.2. Late endosome-to-TGN pathway.....	12
3.1.3. Recycling endosome-to-TGN pathway.....	12
3.2. Retrograde Trafficking and Integrins .....	13
3.3. Index of Trafficking mediating complexes .....	14
3.3.1. Retromer .....	14
3.3.2. Rab GTPases Family .....	14
3.3.3. SNAREs.....	15
3.3.4. GARP complex.....	15
3.3.5. EARP complex .....	15
3.3.6. Sorting Nexins .....	16
4. Autophagy.....	16

<u>Aims</u> .....	19
<u>Results</u> .....	23
1. Confirmation of a putative Golgi-associated trimeric protein complex of Fam91a1, WDR11 and C17orf75 .....	25
2. Fam91a1 and WDR11 KDs impaired retrograde trafficking of Cl-M6Pr and TGN46.....	29
3. Protein synthesis inhibition by cycloheximide shows increased degradation of TGN46 in Fam91a1 and WDR11 KD HeLa cells .....	32
4. Cellular migration and directionality are compromised as $\alpha 5\beta 1$ Integrins are misrouted from FAs at the plasma membrane .....	35
5. Proteomic Mass-Spectrometry screening analysis of knock-downs and Biotin pull-downs of the trimeric complex proteins .....	42
<u>Discussion</u> .....	49
<u>Concluding Remarks</u> .....	59
Materials & Methods.....	63
Bibliography.....	71

## List of figures

<b>Figure A:</b> Representation of the integrin family.....	4
<b>Figure B:</b> Steps of vesicle formation, transport and attaching in Golgi-mediated trafficking events .....	10
<b>Figure 1:</b> Fam91a1, WDR11 and C17orf75 form a trimeric complex .....	26
<b>Figure 2:</b> Confirmation of the Fam91a1, WDR11, C17orf75 complex and its interaction with $\alpha 5$ integrins by BioID .....	28
<b>Figure 3:</b> A-T and H-Q GFP-WDR11 variants localize to the Golgi .....	31
<b>Figure 4:</b> Impaired retrograde Cl-MP6r trafficking in Fam91a1 and WDR11 knock-down cells .....	33
<b>Figure 5:</b> Fam91a1 and WDR11 knock-down reduce TGN46 protein levels and cause an altered intracellular TGN46 localization similar to interfering with the GARP complex absence condition .....	34
<b>Figure 6:</b> Cycloheximide chase Fam91a1 and WDR11 knock-down cells suggest increased degradation kinetics of TGN46 .....	36
<b>Figure 7:</b> siRNA-mediated depletion of GARP and EARP subunits interfere with $\beta 1$ integrin trafficking and recycling back.....	37
<b>Figure 8:</b> Fam91a1 and WDR11 knock-downs interfere with proper $\alpha 5$ integrin trafficking .....	39
<b>Figure 9:</b> Fam91a1 and WDR11 depletion impairs cell migration .....	40
<b>Figure 10:</b> GFP-Fam91a1 re-expression in Fam91a1 depletion HeLa cells does not fully rescue the shFam91a1 migration defect .....	41
<b>Figure 11:</b> Whole Proteome Mass-Spectrometry on control and Fam91a1 and WDR11-depleted HeLa cell lines .....	43
<b>Figure 12:</b> Mass-Spectrometry analysis of the C17orf75 interactome by C17orf75-BioID .....	45
<b>Figure 13:</b> Mass-Spectrometry analysis of the WDR11 interactome by WDR11-BioID .....	46



# **Abstract/Resumo**





## Abstract

Integrin signaling is involved in many aspects of cell function including adhesion, migration through tissues and signaling. Integrin signaling occurs when integrins are extended and ligand bound, and is mediated through interaction of signaling and adaptor proteins to the integrin cytoplasmic tails. The quality of integrin signaling is also influenced by their trafficking through the endosomal system and by their stability. Integrin cytoplasmic domain binding proteins are key to integrin function as integrins do not possess enzymatic activity.

In the previous years the Fässler lab has set up different proteomic approaches to identify proteins that bind to the cytoplasmic domains of  $\alpha 5\beta 1$  integrin including pull-down experiments using the intracellular domains of  $\alpha 5\beta 1$  integrin, proximity-based biotinylation in living cells or adhesome isolation. Among the candidate interactors are proteins that localize to intracellular organelles involved in intracellular trafficking of transmembrane proteins such as the Golgi apparatus and different endosomal proteins. There is increasing evidence that integrin trafficking through the endosomal pathway and retrograde route profoundly affects their function, their 'polarized' distribution on the cell surface, the signaling properties of integrin-associated growth factor receptors and the turnover of ECM proteins such as fibronectin (FN).

The aim of this master thesis is to confirm the interaction of these candidate cytosolic  $\alpha 5\beta 1$  integrin interactors, determine their subcellular localization in the cell and analyze integrin-mediated processes such as cell adhesion, spreading and migration in a loss-of-function situation for these proteins. We started by confirming the existence of a trimeric complex between Fam91a1, WDR11 and C17orf75 at the Golgi which stability is Fam91a1-dependent. This trimeric complex is involved in retrograde trafficking as its depletion impairs transport of Cl-M6Pr and TGN46 to the *trans*-Golgi network (TGN), reduces Cl-M6Pr levels like retromer-depleted cells and compromises TGN integrity. Importantly, the Fam91a1/WDR11/C17orf75 complex is essential for intracellular trafficking of  $\alpha 5\beta 1$  integrin and for effective cell migration. We confirmed the involvement of GARP and EARP complexes in retrograde transport. Finally, proteomic screenings revealed a potential association between

Fam91a1/WDR11/C17orf75 complex and autophagy, endocytic signaling and pubertal development.

Overall the results obtained in this project show that an  $\alpha 5\beta 1$  integrin interacting complex composed of Fam91a1/WDR11/C17orf75 plays a role on TGN-mediated retrograde trafficking of  $\alpha 5\beta 1$  integrin, cell migration and possibly mediate other major cellular processes like autophagy.

**Key words:**

Integrins; *trans*-Golgi network; retrograde trafficking; cell migration; Fam91a1; WDR11; C17orf75; endosomal vesicles;

## Resumo

O processo de sinalização via integrinas está envolvido em muitos aspetos da função celular incluindo adesão, migração através de tecidos e a referida sinalização. Esta sinalização via integrinas ocorre quando possuem uma conformação estendida e estão vinculadas/ligadas a um ligando e essa mesma sinalização é mediada por interações entre as caudas citoplasmáticas das integrinas e proteínas sinalizadoras ou adaptadoras. A eficiência da sinalização por integrinas depende também do seu tráfico através do sistema endossomal e pela sua estabilidade. As proteínas que se ligam ao domínio citoplasmático das integrinas são essenciais para a função das integrinas, pois as integrinas não possuem qualquer tipo de actividade enzimática.

Nos últimos anos passados no laboratório do Dr. Fässler, foram estabelecidas diferentes abordagens de proteómica de forma a identificar poder identificar proteínas que se liguem aos domínios citoplasmáticos da integrina  $\alpha 5\beta 1$ , estes incluem técnicas de pull-down com base nos domínios intracelulares da integrina  $\alpha 5\beta 1$ , como biotinylação de proximidade em células vivas ou isolamento do 'adesoma'. De todos os candidatos que interagem com a integrina  $\alpha 5\beta 1$ , alguns são proteínas que estão localizadas em organelos intracelulares envolvidos no tráfico retrógrado de proteínas transmembranares, como o complexo de Golgi ou diferentes proteínas endossomais. Torna-se cada mais evidente que o tráfico de integrinas pela via endossomal ou via retrograda afetam significativamente a sua função, a sua distribuição polarizada à superfície da célula, as propriedades sinalizadoras de fatores de crescimento associados às integrinas e o turnover de proteínas da matriz extracelular (ECM) como a fibronectina (FN).

O objectivo do trabalho desta tese de mestrado é confirmar as interações de possíveis proteínas citosólicas com a integrina  $\alpha 5\beta 1$ , determinar a sua localização sub-celular e analisar processos que sejam mediados por integrinas tais como, adesão celular, espalhamento e migração em condições de perda-de-função destas mesmas proteínas. Começamos por confirmar a existência de um complexo trimérico entre a Fam91a1, WDR11 e C17orf75 no complexo de Golgi e cuja estabilidade está dependente da Fam91a1. Este complexo trimérico está envolvido no tráfico retrógrado visto que a sua ausência inibe o transporte de Cl-M6Pr e TGN46 para a rede *trans*-Golgi (TGN), reduz

os níveis de CI-M6Pr de forma semelhante a células sem retrómero e compromete a integridade da rede *trans*-Golgi. De relevar que o complexo Fam91a1/WDR11/C17orf75 é essencial para o tráfego intracelular da integrina  $\alpha 5\beta 1$  e para uma migração celular eficiente. Confirmamos o envolvimento dos complexos GARP e EARP no transporte retrógrado. Por fim, screenings da proteômica revelaram uma potencial associação entre o complexo Fam91a1/WDR11/C17orf75 e autofagia, sinalização endocítica e desenvolvimento da puberdade.

No geral, os resultados obtidos neste projeto mostram que um complexo composto por Fam91a1/WDR11/C17orf75 que interage com a integrina  $\alpha 5\beta 1$ , tem um papel muito importante no tráfego retrógrado mediado pela rede *trans*-Golgi da integrina  $\alpha 5\beta 1$ , na migração celular e possivelmente serve de mediador de outros processos celulares chave, como a autofagia.

### **Palavras-chave:**

Integrinas; rede *trans*-Golgi; tráfego retrógrado; migração celular; Fam91a1; WDR11; C17orf75; vesículas endossomais;

# Introduction



# 1. Integrin Overview

Integrin proteins were first characterized 30 years ago as integral membrane proteins. A high number of studies were published laying the foundations on the importance of integrins in several areas of the life science fields. Integrins are specific to the metazoan kingdom of living organisms, as they have not been discovered in any plants, fungi or prokaryotes. They play crucial roles in development, immune responses, leukocyte traffic, hemostasis, cancer cell development and tissue organization processes. As these biological processes are cognate to a multitude of pathological conditions, integrins have long been the target of study for different therapeutic approaches.

Integrins are a major family of cell adhesion receptors mediating adhesion of cells to extracellular matrix (ECM) and to other cells. Additionally, integrins are fundamental in underpinning transmembrane connections to the cell cytoskeleton and particularly, in triggering intracellular signaling cascades through a myriad of different networks.

## 1.1. Integrin Structure

Integrins are non-covalently bonded heterodimers of  $\alpha$  and  $\beta$  subunits. In vertebrates, an assembly of 24 different heterodimers are described from a combination between 18 distinct  $\alpha$  and 8  $\beta$  subunits, which differ in their ligand binding properties, functions and distribution within cells and tissues<sup>1</sup>.

Integrins can be grouped into different subclasses, based on their different ligand-binding properties or subunit composition (Fig. A)<sup>2</sup>. Each of these  $\alpha$  and  $\beta$  subunits contain domains crucial for integrin heterodimerization, that happens before integrins are transported to the cell surface. Each subunit is composed of a large extracellular domain, a transmembrane helix and a shorter cytoplasmic tail. Even though there is no homology between  $\alpha$  and  $\beta$  subunits,  $\alpha$  and  $\beta$  subunits display conserved regions among them<sup>2</sup>.



### 1.1.1. $\alpha\beta$ subunits

The  $\alpha$  subunit is embodied by a seven-bladed  $\beta$ -propeller, connected to thigh and calf domains that together form a 'leg' structure responsible for sustentating the integrin head. These  $\beta$ -propeller blades provide integrins with the ability to bind  $\text{Ca}^{2+}$  and with that to allosterically regulate ligand binding<sup>3</sup>. The  $\alpha$  subunit is the one that grants ligand specificity to integrins.

The  $\beta$  subunit is composed of several domains that, among others, give the integrin heterodimer specific characteristics, including the ability to bind an inhibitory  $\text{Ca}^{2+}$ , an integrin activating  $\text{Mn}^{2+}$  or the cytoskeleton binding site<sup>2,3</sup>. Moreover,  $\beta$  integrin chains have cytoplasmic tails responsible for intracellular ligand-binding, and subsequent activation of downstream signaling pathways, due to a shared NPXY homolog domain<sup>4</sup>.

Non-dimerized single  $\alpha$  and  $\beta$  subunits are not present in the plasma membrane, since  $\alpha$  subunits are the limiting factor for integrin receptor formation as a result of excess  $\beta$  subunits, thus only the dimerized form is present at the cell surface<sup>2</sup>.

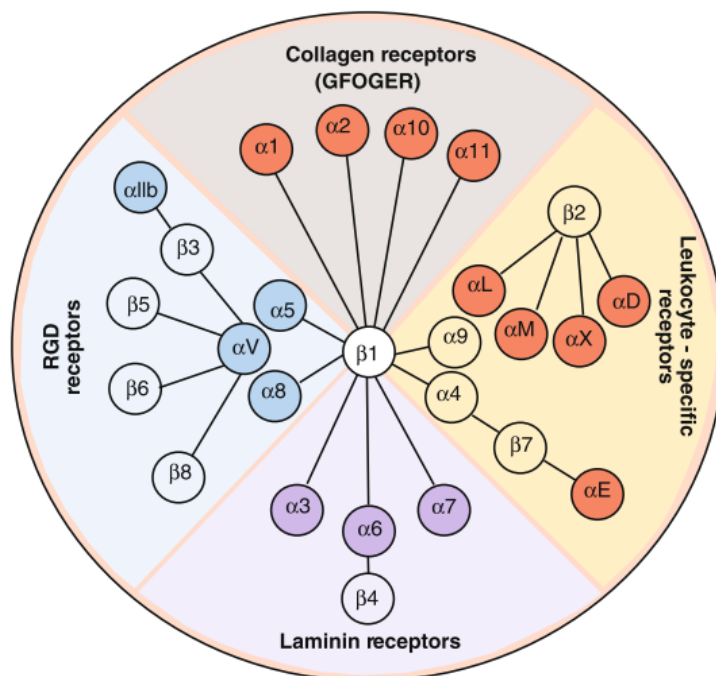


**Figure A** Representation of the integrin family. 24 heterodimers are classified according to their ligand-binding properties or subunit composition.

Adapted from: Barczyk, M., Carracedo, S. & Gullberg, D. Integrins. Cell Tissue Res. 339, 269–280 (2010).

### **1.1.2. Intracellular Domains - Cytoplasmic tails**

Integrin cytoplasmic domains are usually short, contain about 70 amino acids, and while  $\beta$  tails are remarkably homologous, this is opposed to the greatly distinct  $\alpha$  subunit tails<sup>5</sup>. It is thought that the cytoplasmic tails of  $\alpha$  and  $\beta$  subunits form a salt bridge, between the membrane-proximal regions of both chains. This interaction is believed to act as a stabilizer of the integrin inactive and low-affinity state<sup>5</sup>.

The cytoplasmic  $\beta$  tails are comprised of a pair of well-defined motifs, the membrane proximal NPxY and the distal NxxY motifs. These motifs are recognized by proteins containing a phosphotyrosine-binding (PTB) domain including signaling proteins, such as Talin and Kindlin<sup>6</sup>.

### **1.1.3. Transmembrane Domains**

Integrins subunits have a single-spanning transmembrane (TM) domain,  $\alpha$ -helical coiled coil structures of about 25 amino acid residues. Evidence point to the highly conserved GFF motif as critical structure mediating the transition from low-affinity inactive to active states<sup>5</sup>.

### **1.1.4. Extracellular Domains**

The extracellular domains of integrin subunits are composed of a spherical ligand-binding head domain supported by two extended leg domains, that are linked with the rest of the  $\alpha$  and  $\beta$  integrin domains, respectively<sup>5</sup>. The extracellular domain provides the ligand-binding site, that stems from the interaction between  $\alpha$ -chain  $\beta$ -propeller with the  $\beta$ I domain<sup>5,7</sup>.

Most common integrin ligands are components of the extracellular matrix (ECM). Ligand binding elicits conformational changes in the integrin structure after, that leads to integrin activation and signaling (integrin 'outside-in' signaling).

## **1.2. Integrin Signaling and Function**

Contrary to most of other transmembrane receptors, integrins have the ability to signal bidirectionally. This means that integrins transduce signals from the extracellular

environment following ligand binding to promote intracellular changes ('outside-in signaling') but intracellular stimuli can also elicit extracellular responses ('inside-out signaling')<sup>4</sup>.

During inside-out activation of integrins, intracellular signaling pathways lead to the binding of talin and kindlin to the  $\beta$  integrin cytoplasmic tails inducing a conformational change in the transmembrane and cytoplasmic integrin domains that is transmitted to the extracellular domain. The extracellular domain changes from a bent, low-affinity, inactive conformation to an extended high-affinity ligand-binding conformation<sup>8</sup>.

Integrins do not have catalytic activity, integrin activation increases affinity for ECM ligands, but to activate intracellular signaling pathways activated integrins are needed to cluster and recruit cytoplasmic proteins to their tails. Nascent adhesions are formed, that evolve to focal complexes, then larger focal adhesions (FA) and finally, fibrillar adhesions<sup>4</sup>. Ligand-binding events to the extracellular head-domain of integrin, initiate the previously described step-wise assembly of a dynamic multiprotein complex (focal adhesion), that serve as the hub for transmission of intracellular signals (outside-in signaling)<sup>4,5</sup>.

These mechanisms are essential for the cell-adhesion receptor properties of integrins, that mediate cytoskeletal rearrangements, up- and downregulate cascade pathways and change gene expression. All of this influences processes like survival, growth and differentiation of cells<sup>4</sup>.

### **1.3. $\alpha 5\beta 1$ Integrin and Cell Migration**

$\alpha 5\beta 1$  integrin, a major fibronectin (FN)-binding receptor, interacts with the tensin adaptor protein to drive the formation of long and stable fibrillar adhesion complexes<sup>9,10</sup>. Active  $\alpha 5\beta 1$  integrin is an endocytic FN receptor that plays a major role in regulating FN fibrillar matrix<sup>11</sup>. The fibronectin binding to differently distributed  $\alpha 5\beta 1$  integrins at the cell surface, stimulates RhoA-mediated organization of cell matrix adhesion<sup>12</sup>. The activation of RhoA signaling is tightly linked to  $\alpha 5\beta 1$  recycling, as the recycling dictates the availability of the heterodimer at the cell surface and subsequent random cell migration<sup>4</sup>.

Cell migration is a highly complex process composed of a myriad of aggregated and organized steps<sup>13</sup>. During migration, forces are generated to drive the protrusions of the leading edge forward across the ECM. Followed by the formation of adhesion sites at the protrusions, adhesions at the back of the cell will be disrupted to move of cell body<sup>13,14</sup>.

Integrins, including  $\alpha 5\beta 1$ , are primary components of the adhesion complexes that serve as traction points that enable cell movement and also integrate signals that regulate the migration process<sup>15</sup>.

## 2. Integrin Trafficking

As indicated above, integrin-mediated processes operate under tightly regulated signaling events. Integrin availability at the plasma membrane is paramount for proper physiological function and homeostasis.

Cell surface integrin availability is regulated by several trafficking mechanisms. Simply put, cycles of endocytosis, re-exocytosis (recycling) or degradation, control the pool of available integrins at the plasma membrane. For some integrins, their clearance from the plasma membrane can be as fast as 30 minutes. Interestingly, the half-life of an integrin is around 12-24 hours, which means that most of the integrins are continuously being recycled back to the plasma membrane<sup>16</sup>. These mechanisms are dependent on the function of several regulators like kinases, cytoskeleton modulators, Rab family GTPases and Arf family GTPases.

### 2.1. Canonical Trafficking

Integrins are endocytosed by clathrin-dependent and -independent routes, as the latter include macropinocytosis, actin-rich projections or clathrin-independent carriers<sup>17</sup>. The internalization is followed by sorting mechanisms that decide if are to be either recycling back to the cell surface or sorted into a degradative pathway. One integrin heterodimer can, at different cell stages, follow different internalization paths or more than one recycling route. For example,  $\alpha 5\beta 1$  can be endocytosed either in a clathrin- or caveolin-dependent manner.

### **2.1.1. Clathrin-dependent endocytosis of integrins**

Specific motifs at the integrin cytoplasmic  $\beta$ -subunit tails facilitate their recruitment of to clathrin-coated structures through interactions with adaptor proteins like AP2 and PTB-containing Dab and Numb, as well as bridging proteins such as HAX1 and cortactin<sup>18</sup>. Dab2 was found to be an alternative clathrin adaptor of  $\beta$ 1 integrins that regulates, along with dynamin 2, microtubule-driven focal adhesion disassembly followed by endocytosis.

It became evident the role of Dab2 in clathrin-dependent endocytosis, despite of the unclear results of whether all conformation states of integrins are endocytosed or just the active conformation. Recent literature also reported the requirement of a motor protein, myosin VI, in the endocytosis of  $\alpha$ 5 $\beta$ 1 integrin-NRP1 complexes from fibronectin-rich fibrillar adhesions along F-actin structures<sup>18</sup>. Altogether, it was established the role of clathrin-mediated endocytosis in focal adhesion disassembly<sup>19</sup>.

### **2.1.2. Clathrin-independent endocytosis of integrins**

Some integrins including  $\alpha$ 5 $\beta$ 1 can follow more than one route of internalization. Overexpression of Rab21, led to an alternative endocytosis route using caveolin-1-containing structures (caveolae). In these cells, caveolin-1 depletion resulted in an accentuated reduction of  $\beta$ 1 and fibronectin endocytosis indicating how clathrin-independent endocytosis can regulate fibronectin matrix turnover and ECM remodelling<sup>20</sup>. However, the molecular mechanisms of this route are still poorly defined, and needs further analysis to enable a full understanding of the integrin endocytosis process.

### **2.1.3. Recycling: Short-loop pathway**

The Rab4 fast-recycling pathway ('short-loop') is one of two spatially and temporally defined mechanisms of recycling<sup>21</sup>. Being associated to early endosomes, the entry to this route is controlled by Rabex-5 (Rab5 guanine-exchange-factor (GEF)) that activates Rab5, and by Rabaptin-5 that promotes a link between Rab5 and Rab4.

Phosphorylation of Rabaptin-5 by PKD1 controls Rabaptin-5 association to Rab4 endosomes which contain  $\alpha$ v $\beta$ 3 integrins, allowing the integrins to recycle back to the

plasma membrane. Thus, this route provides newly assembling adhesions with  $\alpha\beta3$  integrins, stimulating persistent cell migration on low fibronectin environments<sup>22</sup>. Overall it is established that Rab4/5 early endosome-recycling of  $\alpha\beta3$  and inactive  $\beta1$  integrins, allows cells to drive path persistent migration (in FN environments) and invasion of cancer cells<sup>22</sup>.

#### **2.1.4. Recycling: Long-loop pathway**

The long-loop pathway is mainly characterized by Rab11-positive vesicles that go through the perinuclear recycling compartment (PNRC) prior to returning to the cell surface<sup>17</sup>.

Different signaling pathways promote selectivity in Rab11-mediated recycling of a multitude of different integrin heterodimers, and therefore regulating cell migration<sup>21</sup>. Evidences showed that PKB/Akt acts by phosphorylation of GSK-3 $\beta$ , to selectively recycle  $\alpha5\beta1$  and  $\alpha\beta3$  via Rab11-positive compartments<sup>23</sup>. It was also reported that the ADP ribosylation factor GTPase 6 (Arf6) present in the PNRC paires with Rab11 to regulate the exit of  $\beta1$ ,  $\alpha5\beta1$  and  $\alpha\beta3$  integrin from the PNRC, and cell migration towards fibronectin<sup>21,24</sup>. Moreover, when Rab11 effector Rab-coupling protein (RCP) binds  $\alpha5\beta1$  integrin, signals cells for rapid and random cell migration<sup>25</sup>.

In summary, these studies demonstrate a step-wise controlled mechanism of integrin transport through different recycling routes.

### **3. Golgi-mediated Trafficking**

The Golgi apparatus is a central organelle of utmost importance when it comes to protein sorting and trafficking in eukaryotic cells. The Golgi-mediated trafficking is characterized by a bidirectional vesicular transport between different cellular compartments<sup>26</sup>. This vesicular transport can be divided into the biosynthetic/secretory pathway from the endoplasmic reticulum (ER) to the plasma membrane (anterograde trafficking) or the reverse route, from the endosomal system/plasma membrane back to early compartments (retrograde trafficking)<sup>27</sup>. These two trafficking routes can be

fragmented into five main steps: budding, movement, tethering, docking and fusion (Fig. B)<sup>28</sup>.

Anterograde movement from the ER to the Golgi and retrograde movement from the Golgi back to the ER, are mediated by coatamer coating protein-coated vesicles, COPI and COPII respectively<sup>29</sup>. The pathways are connected and when COPII-dependent retrograde transport is impaired, COPI-dependent anterograde transport is also compromised due to the fact that tethering factors and cargo receptors are depleted from the ER<sup>29</sup>. This demonstrates a tight relation between both trafficking pathways.

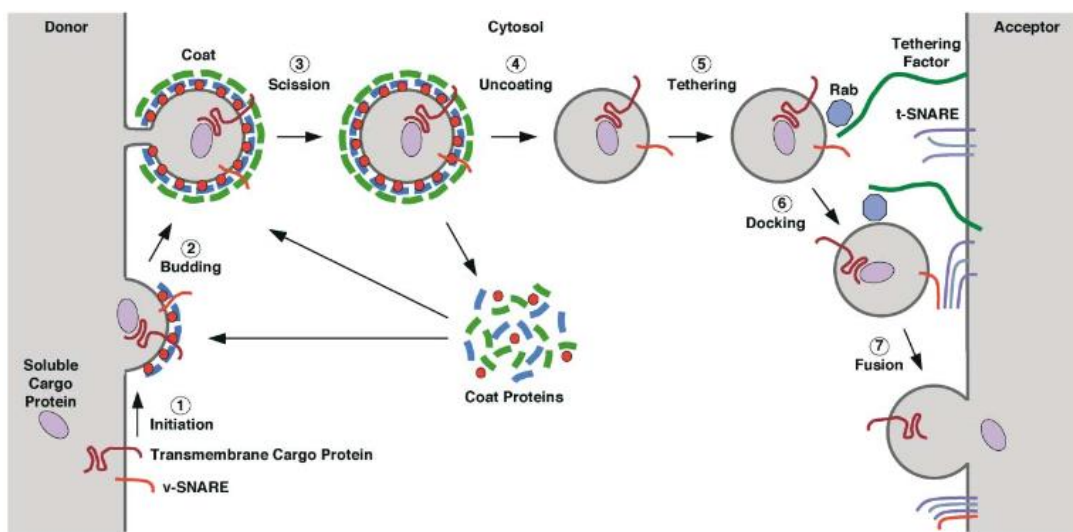


**Figure B** Steps of vesicle formation, transport and attaching in Golgi-mediated trafficking events.

Adapted from: Bonifacino, J. S. & Glick, B. S. The Mechanisms of Vesicle Budding and Fusion. *Cell* **116**, 153–166 (2004).

### 3.1. Retrograde Trafficking and the *trans*-Golgi network

Transport of proteins from the endosomal system/plasma membrane to the *trans*-Golgi network (TGN), Golgi membranes (*cis*-, medial- and *trans*-Golgi) or even to the endoplasmic reticulum (ER) is known as retrograde transport<sup>27,30</sup>. This retrograde route is also sometimes hijacked by pathogens and toxins in order to promote cytotoxicity or gain control of the cells (Shiga toxin, cholera toxin, ricin and herpes virus)<sup>31–33</sup>. Thus, understanding this trafficking route and the proteins involved will unveil new possible outlets for upcoming therapeutic approaches and drug delivery strategies.

Amongst all of the framework in which retrograde trafficking takes place, the *trans*-Golgi network has a central role as a traffic hub that regulates both the secretory

pathway and the retrograde route. As the anterograde transport depletes sorting receptors, enzymes and vesicle-fate targeting factors from the Golgi these proteins need to be retrieved to the TGN to allow for continuous cell function. There are three main retrograde transport routes characterized, referred to as early, recycling and late endosome-to-TGN pathway. Each of these retrograde pathways is characterized by different composing machineries and cargos, like the mannose 6-phosphate receptors (MPRs)<sup>34</sup> or transmembrane proteins<sup>35</sup>.

Endosomes are a complex mosaic membrane system composed of tubules and vesicles, that give rise to early/late endosomes, lysosomes and the endocytic recycling compartment (recycling endosomes)<sup>36</sup>. Yet, all of these structures are part of a continuum dependent on maturation stages, rather than defined singular structures, sometimes distinguishable only by their morphology<sup>37</sup>. Therefore, classification of endosome-to-TGN transport into three separate and distinct pathways is not a 100% reliable approach but nonetheless still required to further our understanding of the retrograde trafficking system.

### **3.1.1. Early endosome-to-TGN pathway**

This pathway was first discovered as the pathway exploited by Shiga toxin (STxB)<sup>38</sup>, and later found to be the route traversed by MPRs, which are dependent on AP1 and PACS-1 (clathrin adaptors), clathrin coating and the retromer complex<sup>37</sup> for their movement.

The retromer is a phylogenetically conserved multisubunit complex, whose best characterized cargo is the cation-independent mannose 6-phosphate receptor (CI-M6Pr). The CI-M6Pr binds freshly synthesized acid hydrolases at the TGN. These acid hydrolases are then transported to the early endosomes/pre-lysosomal compartment (part of the endosomal continuum), before pH acidic-induced release and proteolytical cleavage into active form at the lysosomes<sup>30,34</sup>. Then, the retromer acts to retrieve these CI-M6Prs back to the TGN, so they can re-engage in a new cycle of acid hydrolase sorting.

Conjointly, the Golgi-associated retrograde protein complex (GARP) was also shown to be necessary for proper retrograde trafficking of CI-M6Pr, as well as STxB and TGN46 (TGN transmembrane protein), to the trans-Golgi network<sup>39,40</sup>. Moreover, the



recruitment of the GARP complex at the TGN is promoted by Rab6 GTPase<sup>39</sup> which in turn enables SNARE complex formation.

The SNARE complexes are another set of proteins that are cycled between the TGN and the endosomes. There are two distinct SNARE complexes, vesicle-membrane SNAREs (v-SNAREs) which flow from the TGN to the early endosome in vesicles and mediate the membrane fusion of these vesicles with the endosome compartments. The fusion happens through assembly with the second type of SNAREs, the endosomal target-membrane SNAREs (t-SNAREs)<sup>41</sup>. After the fusion process is complete, the v-SNARE-t-SNARE complex (SNAREpin) is disassembled, and the v-SNAREs (Snc1) are retrieved in retrograde transport vesicles back to the TGN in a GARP-dependent fashion<sup>30,40</sup>.

### **3.1.2. Late endosome-to-TGN pathway**

Late endosomes were also proposed to be a source of MPR as retrograde cargos for the TGN. In this case, CI-M6Pr retrograde flow is mediated by a different complex of proteins, the Rab9-TIP47 duplex.

Rab9 is a member of the large family of Ras-like GTPases that regulates vesicular transport events at the level of membrane targeting, and localizes primarily at the surface of late endosomes<sup>42</sup> and vesicles that bud from them to fuse with the TGN<sup>30</sup>. GTP-bound Rab9 forms pairs with TIP47, Rab9 serves as the membrane-recruitment component, while TIP47 acts as a cargo-recognition component since it binds the cytosolic domain of CI-M6Pr<sup>30</sup>. Interestingly, this Rab9-TIP47-duplex-derived retrograde transport of CI-M6Pr is also dependent on a specific syntaxin 10 SNARE complex. Knock-down of syntaxin 10 does not inhibit early transport of known endosome-to-TGN cargos (TGN46/cholera toxin) but not MPRs, showing the specificity of certain factors for different endosome-to-TGN pathways.

### **3.1.3. Recycling endosome-to-TGN pathway**

Not many cargos have been reported to go through the recycling endosome-to-TGN, yet CI-M6Pr and Shiga toxin need the recycling endosome-to-TGN pathway for efficient transport, in addition to the early endosome-retromer-mediated transport<sup>43</sup>.

Furthermore, v-SNARE VAMP4 was shown to be trafficked from early and recycling endosomes, which goes in hand with the fact that VAMP4 forms a SNARE complex (SNAREpin) with other known retrograde transport t-SNAREs: syntaxin 6 (Stx6), syntaxin 16 (Stx16) and Vti1a<sup>44</sup>.

A recent paper characterized a newly found complex that operates at the level of recycling endosomes. This complex called, the endosome-associated recycling protein (EARP), is a multisubunit tethering complex with composition very similar to the TGN-localized docking complex GARP<sup>45</sup>. While GARP complex is composed of Ang2 (Vps51), Vps52, Vps53 and Vps54<sup>39</sup>, this new tethering complex EARP contains syndetin (Vps50) instead of Vps54.

Although EARP complex was not directly shown to mediate a recycling endosome-to-TGN pathway, multisubunit tethering complexes normally promote SNARE-mediated vesicle fusion<sup>46</sup>, suggesting that indeed EARP (and to some extent GARP) is mediating vesicle transport event from a distinct site to another. Adding that shared subunits of EARP and GARP (Ang2, Vps52 and Vps53), were discovered to hold interactions with Stx6–Stx16–Vti1a–VAMP4 complex<sup>45</sup> (recycling endosome-to-TGN-associated SNAREpin complex mentioned above), it is likely that EARP also mediates the trafficking events of recycling endosomes-to-TGN. Sustaining this, is the observation of a small population of GARP localized in the recycling endosomes, which like CORVET-to-HOPS complex-mediated early-to-late endosome conversion, which suggests that EARP might be a product of conversion after GARP reaches the recycling endosomes<sup>47</sup>.

### **3.2. Retrograde Trafficking and Integrins**

The link between retrograde transport and integrin trafficking is still very much unexplored. So far, the most commonly studied integrin trafficking pathways are the canonical Rab4-dependent short-loop and Rab11-dependent long-loop pathways<sup>48</sup>.

However, a recent study found that cell adhesion, persistent cell migration, polarized distribution of  $\beta$ 1 integrin and focal adhesion disassembly dynamics depend on a functional retrograde route<sup>49</sup> indicating that TGN-mediated retrograde transport of non-ligand-bound  $\beta$ 1 integrin heterodimers acts as a complementary recycling

pathway. As a consequence, major cell functions that rely on integrin trafficking, might also be dependent on retrograde trafficking.

### **3.3. Index of Trafficking mediating complexes**

Here I give a concise insight about some of the most important and best studied complexes involved in the retrograde trafficking network.

#### **3.3.1. Retromer**

The retromer is a multisubunit heteropentameric complex composed of sorting nexin dimer (SNX1-SNX2) and vacuolar sorting protein trimer (VPS26 -VPS29-VPS35) in humans. One of its most described functions is the retrieval of acid hydrolase receptors (MPRs) to the trans-Golgi network, in retrograde transport<sup>30</sup>. The retromer associates with the cytosolic interface of endosomes coated with clathrin. The SNX dimer is responsible for the recruitment of the retromer to endosomes, while the VPS trimer mediates the cargo-recognition process to recruit transmembrane proteins from vacuole endosomes and channeling them for recycling at the TGN<sup>50,51</sup>.

#### **3.3.2. Rab GTPases Family**

Rab proteins compose one of the largest families of monomeric small GTPases, thought to be more than 63 members in humans<sup>52</sup>. Their function as regulatory proteins are based mainly on their ability to act molecular switches that shuffle between GTP- GDP-bound conformations. While GTP-bound is the active form and the GDP-bound the inactive one, their special feature lies in the ability to cycle between these active/inactive states, enabling a temporal and spatial regulation of membrane transport. They are characterized by a highly structural heterogeneity, thus endowing them with very selective activity regarding their effectors. The diversity of Rab effectors is obvious during intracellular transport, where they can mediate processes like budding, movement, tethering, docking and fusion of vesicles into target compartments. This sets up Rab proteins as pivotal factors in controlling a multitude of intracellular processes<sup>52</sup>.

### **3.3.3. SNAREs**

SNAREs (soluble *N*-ethylmaleimide-sensitive factor attachment protein receptors), have a crucial role in the docking and fusion events of vesicle-mediated transport into target compartments. Regarding their function, they can be divided into v-SNAREs, associated with vesicles being transported, and t-SNAREs which are associated with the targeted receiving compartment. Binding of v-SNARE to a specific t-SNARE leads to the formation of the trans-SNARE/SNAREpin complex. This SNARE complexes function are important for secretory, endocytic and retrograde pathways as they mediate fusion events at the TGN, early/recycling endosomes, or even mediate fusion of lysosomes with the plasma membrane<sup>30,41</sup>.

### **3.3.4. GARP complex**

The Golgi-associated retrograde protein (GARP) complex, is a tethering/docking complex mainly localizing to the TGN, the sorting station of the cell composed of four subunits (Ang2 (VPS51), VPS52, VPS53 and VPS54). Its recruitment to the TGN is achieved by interactions with Rab6, where it coordinates tethering and fusion of vesicles, due to interaction with t-SNARE Tlg1<sup>53</sup>. The GARP complex is known for the retrieval of receptors for lysosomal hydrolase precursors, such as the mannose 6-phosphate receptors (MPRs) and interfering with GARP function results in impaired retrograde transport to the TGN of transmembrane proteins (TGN46 and Kex2), SNAREs (v-SNARE Snc1), toxins (Shiga toxin, ricin) and lysosomal dysfunction from the impaired maturation of hydrolase precursors<sup>47,54</sup>. Hence, GARP plays a vital role in endosome to TGN transport in a wide range of cellular functions.

### **3.3.5. EARP complex**

The endosome-associated recycling protein (EARP) is a tethering complex with a similar subunit composition as the GARP complex, with the exception of an exchange of syndetin (VPS50) for VPS54. Syndetin is the key subunit that determines its distinct localization to recycling endosomes instead of the TGN, like the GARP complex. Its main function was described as a tethering factor for recycling proteins from the endosomes to the plasma membrane. EARP promotes the recycling of transferrin receptor (TfR) back to the cell surface, presumably through tethering of endosomal SNAREs. EARP also

associated Rab4-positive recycling endosomes (short-loop recycling pathway), and thus established a requirement of multisubunit tethering complexes in the recycling endocytic pathway<sup>29,45,47</sup>.

### 3.3.6. Sorting Nexins

Sorting nexins are a class of proteins containing a phox-homology (PX) domain, and up to 33 have been identified in mammals. They bind phosphatidylinositol-3-monophosphates (PtdIns3P) and function in processes such as endocytosis and endosomal sorting/signaling<sup>55</sup>. Their main function is the orchestration of cargo sorting in the membranous intricacy of the endosomal network. One of the best studied roles of sorting nexins is within the retromer complex (SNX1-SNX2 dimer). After internalization, early endosomes can sort their cargo either for lysosomal degradation, to downregulate signaling receptors, or recycle it back to the plasma membrane. This retrieval of the cargo is often coordinated by sortin nexins<sup>56</sup>. For instance, the binding of SNX17 and SNX31 to the NPXY motif of the  $\beta$ 1 subunit cytoplasmic tail of  $\alpha$ 5 $\beta$ 1 integrin at the early endosomes, prevented lysosomal degradation resulting in its recycling back to the plasma membrane<sup>57,58</sup>.

## 4. Autophagy

Within all of the catabolic pathways available for a cell, autophagy is the most severe. During autophagy, organelles and proteins are confined in acidic vacuoles for massive lysosomal degradation. This pathway can be part of the response to nutrient deficit, cell death, cell survival, development or tumor suppression<sup>59</sup>.

Autophagy starts with the formation of a double-membrane vacuole or autophagosome, which requires the function of a crucial family of autophagy-related proteins (ATGs). A complex containing ATG14 and Beclin-1 is recruited to the endoplasmic reticulum (ER) and acts upstream of the ATG12-ATG5-ATG16L1/LC3 elongation system. This complex along with ATG8 is responsible for elongating and closing the autophagosomal membrane<sup>60,61</sup>.

Moreover, autophagy fulfils numerous functions and regulates a multitude of physiological processes including cell migration, yet little is known how autophagy affects integrin-mediated cell migration on a molecular level. There are apparent contradictory observations of this phenomenon. For instance, one study showed that increased cell migration is associated with low levels of autophagy, by reducing endocytic recycling of integrins in HeLa cells<sup>62</sup>. While another study showed that reduced levels of autophagy correlated with reduced tumor cell migration, due to disruption of focal adhesion disassembly<sup>63</sup>. Further research is needed to fully uncover the mechanisms by which autophagy regulates integrin-mediated processes.



# Aims





## Aims

The aim of this thesis was to characterize three novel candidate cytosolic  $\alpha 5\beta 1$  integrin interactors for their roles in the regulation of  $\alpha 5\beta 1$  integrin stability and/or trafficking.

Specifically it was aimed to

- Confirm the interaction of candidate  $\alpha 5\beta 1$  integrin interactors.
- Determine the subcellular localization of candidate  $\alpha 5\beta 1$  integrin interactors and their co-localization with  $\alpha 5\beta 1$  integrin.
- Analyze the knockdown cell lines for alterations in integrin-mediated processes such as cell adhesion, spreading and migration.



# Results



## **1. Confirmation of a putative Golgi-associated trimeric protein complex of Fam91a1, WDR11 and C17orf75**

Previous reports<sup>33,64</sup> and previous proteomics in the Fässler department (unpublished data) suggested the existence of a putative trimeric complex between Fam91a1, WDR11 and C17orf75. To further investigate this complex, we performed co-immunoprecipitation (co-IP) assays of WDR11 and Fam91a1 in HeLa cells (Fig. 1a,b). Immunoprecipitation of WDR11 co-immunoprecipitated both Fam91a1 and C17orf75 in control shRNA (shCtr) HeLa cells, but not in the shRNA-mediated WDR11 knock-down cells (Fig. 1a). Furthermore, both C17orf75 and WDR11 were co-immunoprecipitated with an antibody against Fam91a1 but when a control IgG (Fig. 1b). These experiments demonstrate the existence of a trimeric complex between Fam91a1, WDR11 and C17orf75.

To assess the subcellular localizations of Fam91a1 and WDR11 with organelle markers, knock-down cells for either Fam91a1 or WDR11 were used for immunofluorescence assays. As expected from previous experiments, which showed a localization of WDR11 to the TGN (unpublished data and ref.4), we observed both Fam91a1 and WDR11 in the vicinity of the cis-Golgi marker GM130<sup>65</sup> (Fig. 1c,d: shCtr). Interestingly, the WDR11 signal was highly reduced in Fam91a1 knock-down cells similarly to WDR11-depleted cells, and we did not observe a Golgi localization and expression, while Fam91a1 localization and expression remained unaltered in WDR11 knock-down cells compared to control (Fig. 1 c,d: shFam91a1; shWDR11). These findings were substantiated via western blot analysis, in which we observed that Fam91a1, WDR11 and C17orf75 were all reduced in Fam91a1 knock-down cells, while the levels of Fam91a1 and C17orf75 remained unchanged in WDR11 knock-down cells (Fig. 1e).

This suggests that the trimeric complex might be Fam91a1-dependent, and that Fam91a1 knock-down leads to reduction of WDR11 protein rather than its mislocalization from the Golgi apparatus.

To confirm the immunoprecipitation results with an independent method we made use of BioID. BioID is a proximity-dependent biotin identification assay, based on a promiscuous biotin ligase which labels proteins that are in its close proximity<sup>66</sup>. Cells stably expressing either C17orf75- or  $\alpha$ 5-BioID-HA fusion proteins, previously reported

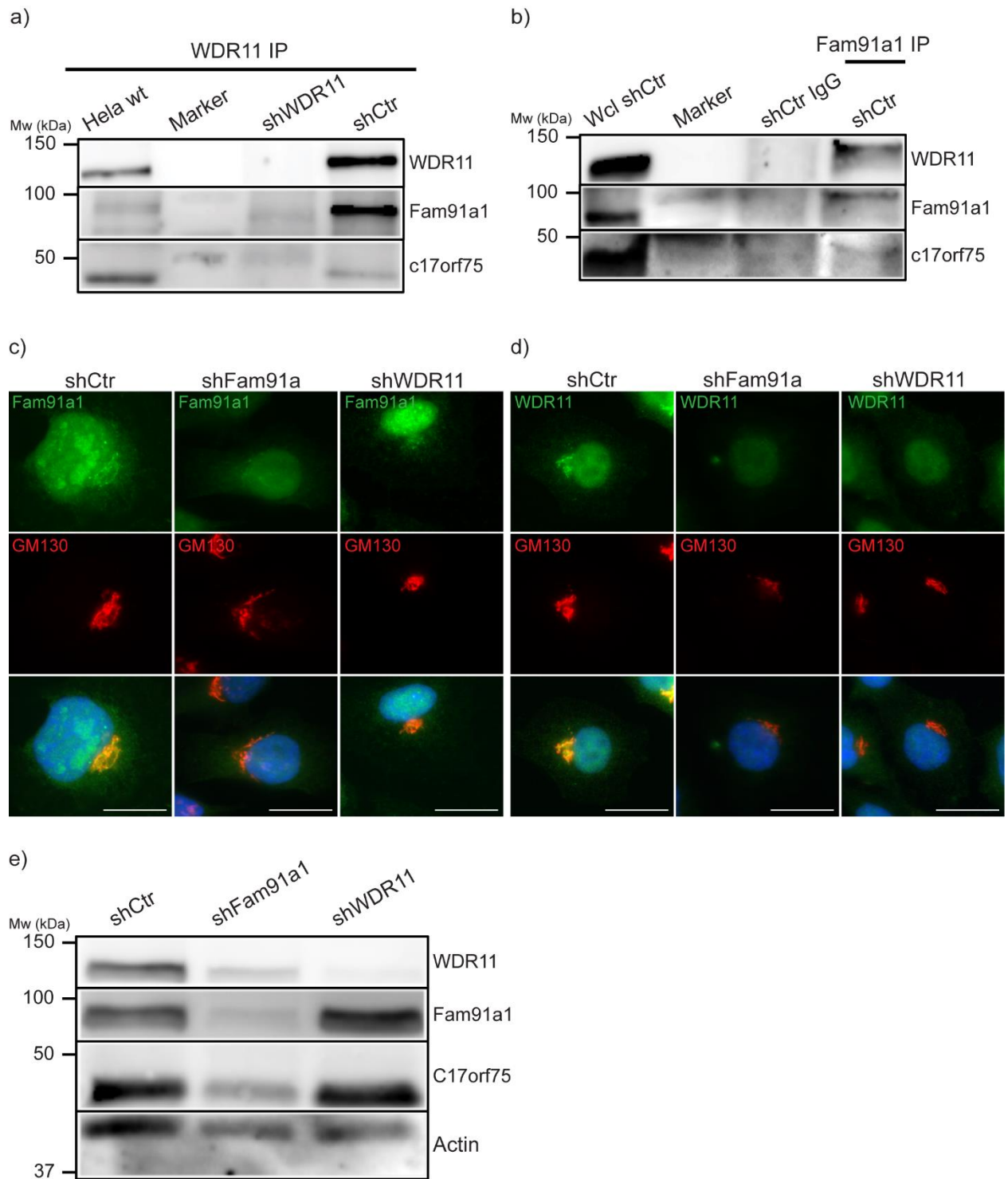


**Figure 1** Fam91a1, WDR11 and C17orf75 form a trimeric complex. **(a,b)** Co-immunoprecipitation of the putative trimeric complex proteins in HeLa cells by with antibodies against WDR11 cells **(a)** and against Fam91a1 **(b)** in the indicated HeLa cell lines. Wcl, whole-cell lysate. Immunoblotted with antibodies against WDR11, Fam91a1 and C17orf75 antibodies. **(c,d)** Immunostaining of fixed shCtr, shFam91a1 or shWDR11 HeLa cells plated on fibronectin-coated cover-slips, confirming the knock-down and showing WDR11 stability dependency on Fam91a1. Immunolabeled with antibodies against cis-Golgi marker GM130 (red) and Fam91a1 (green) **(c)** or WDR11 (green) **(d)**. The immunostaining images were acquired by fluorescence microscopy. Nuclei were counterstained with DAPI (blue). **(e)** Western-blot confirming absence of WDR11 and C17orf75 in shFam91a1 knock-down cells. Scale bars, 100  $\mu$ m.

to be retrogradely transported through the Golgi<sup>49</sup>, proteins were untreated or incubated in the presence of biotin (100  $\mu$ M) over night, fixed and immunostained against HA-tag and Streptavidin-Cy3 to detect biotin. While C17orf75-BioID fusion protein localized to a peri-nuclear position reminiscent of the Golgi in shC17orf75 cells, the  $\alpha$ 5 integrin fusion protein localized to focal adhesion (FA) structures (Fig. 2a). When stained against biotin using fluorescently-labeled streptavidin, we observed a signal in cells after biotin treatment, in the vicinity of the BioID fusion proteins, indicating that the BioID proteins are functionally active (Fig. 2b).

Next we treated cells with or without 100  $\mu$ M biotin overnight, lysed the cells and performed a Streptavidin pulldown of C17orf75 and  $\alpha$ 5 integrin-BioID constructs. Immunoblots showed that the C17orf75 construct was able to co-precipitate all three endogenous proteins (Fig. 2c), whereas  $\alpha$ 5 integrin construct showed very weak binding for WDR11 and Fam91a1 (Fig. 2d). This data confirms the interaction of Fam91a1, C17orf75 and WDR11 to form a trimeric, and the interaction of that complex with  $\alpha$ 5 integrin likely at the Golgi, at some point of the  $\alpha$ 5 integrin trafficking events.

Various heterozygous missense variants in the WDR11 gene were identified in IHH and KS patient's genotypes<sup>67</sup>. To determine if the WDR11-depleted cells, when rescued with these point-mutated forms of WDR11, still co-localized with cis-Golgi. We transiently expressed GFP-WDR11 constructs containing point-mutations (A435T; H690Q; or HH507/513AA), in either WDR11 knock-down or WT HeLa cells. By co-immunostaining WDR11 with GM130 antibodies, we observed that in shWDR11 cells, the A435T (A-T), H690Q (H-Q) and HH507/513AA (HH-AA) mutated constructs still properly localized to the Golgi apparatus (Fig. 3a). Then, performing a WB in the same conditions with a GFP antibody, only (A-T) and (H-Q) constructs displayed GFP bands, validating the immunostainings results (Fig. 3b).

Since (HH-AA) did not show any GFP presence in the WB, no conclusions can be drawn of either the WB or the immunostainings regarding that mutation effect (Fig. 3b).



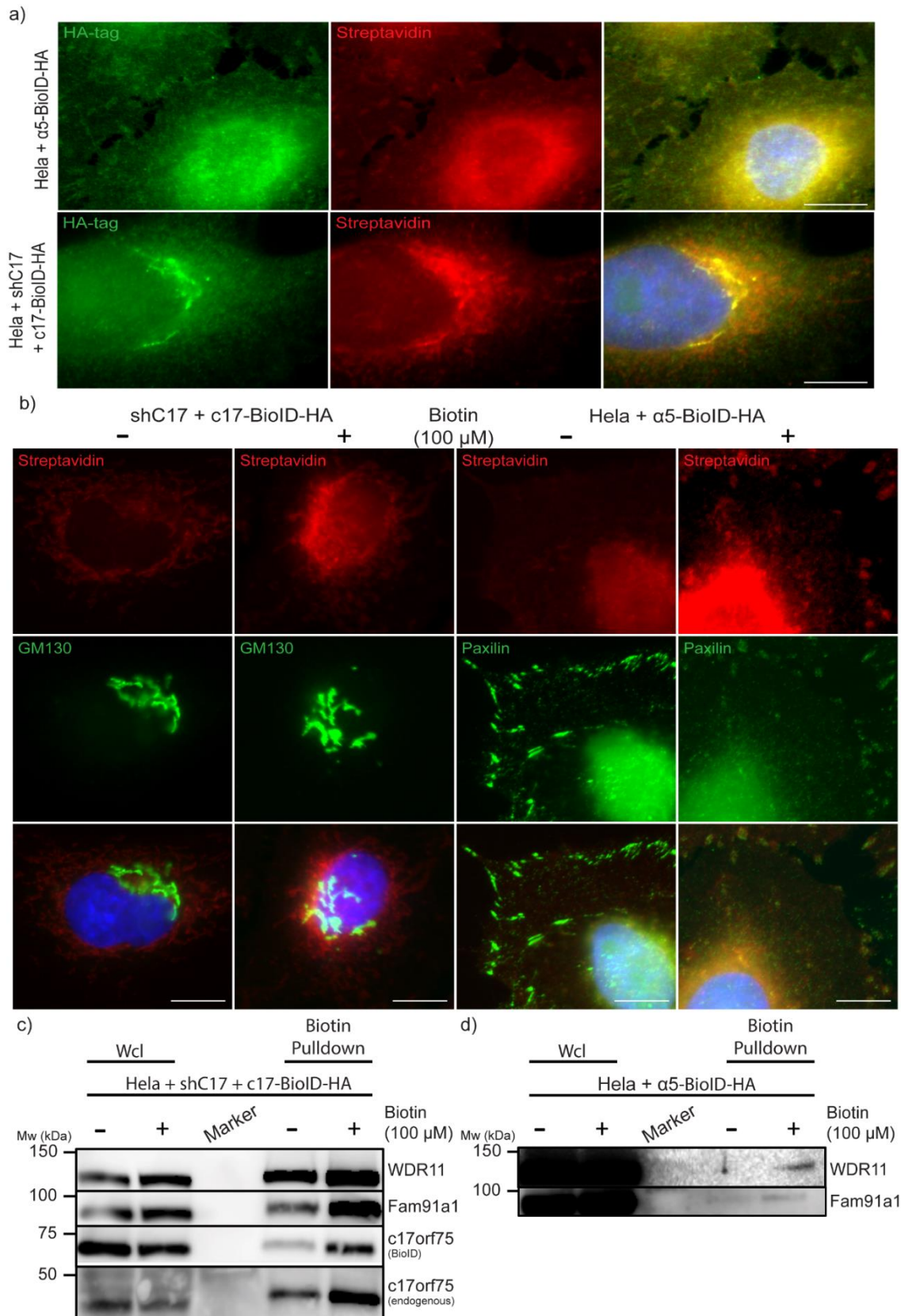


**Figure 2** Confirmation of the Fam91a1, WDR11, C17orf75 complex and its interaction with α5 integrins by BioID (a,b) Co-localization of biotinylated proteins (labeled by Streptavidin-Cy3, red) with the BioID fusion

proteins in HeLa cells stably expressing C17orf75-BioID-HA or  $\alpha 5$ -BioID-HA in the presence of biotin (100  $\mu$ M). BioID-fusion proteins were detected with a HA-tag antibody (green) **(a)**. To define the subcellular localization cells in **(b)** we co-stained with antibodies against GM130 or Paxilin (green) in the presence or absence of biotin. Scale bars, 200  $\mu$ m (a) and 100  $\mu$ m (b). Nuclei were counterstained with DAPI (blue)..Scale bars, 200  $\mu$ m (a) and 100  $\mu$ m (b). Nuclei were counterstained with DAPI (blue) **(c,d)**.

Formation and localization of the trimeric complex proteins in Golgi and focal-adhesions, its interaction with  $\alpha 5$  integrin was determined by BioID in biotinylation, followed by biotin pull down and western-blot analysis of the neighboring partners of cells expressing the BioID fusion protein with Cc17orf75 **(c)** or  $\alpha 5$  integrin **(d)**.

## **2. Fam91a1 and WDR11 KDs impaired retrograde trafficking of CI-M6Pr and TGN46**

Since the Fam91a1/WDR11/C17orf75 complex localizes to the TGN (unpublished), we sought to investigate and establish a functional connection between our trimeric complex and TGN-mediated trafficking, a major vesicle and protein sorting center as it is part of the anterograde and retrograde transport pathways<sup>68</sup>. For this, we investigated the expression levels and the distribution of cation-independent mannose 6-phosphate receptor (CI-M6Pr), a known cargo that is transported from the endosomes/lysosomes to vesicles and if proteins of the retrograde transport are inhibited, CI-M6Pr is mislocalized within cells which can lead to degradation<sup>30,68,69</sup>. Through an immunostaining assay we examined CI-M6Pr signal and localization with two ways, either after fixation and permeabilization or we followed CI-M6Pr trafficking in living cells.

To determine if CI-M6Pr expression levels were altered in a Fam91a1 or WDR11 knock-down situation, we stained the cells for CI-M6Pr and analyzed the stainings by fluorescent microscopy by keeping the exposure times constant. In both cases of antibody incubation, a significant decrease in immunofluorescence signal of the mannose-6-phosphate receptor was observed in shFam91a1 and shWDR11 HeLa cells as compared to control cells (Fig. 4a: = T exposure). However, we not only detected a decrease in CI-M6Pr expression but also noticed a difference in CI-M6Pr distribution within the cell. The remaining CI-MP6r in the Fam91a1 and WDR11 knock-down cells exhibited a scattered small vesicle cytoplasmic distribution while a strong Golgi staining was observed in control cells (Fig. 4a:  $\neq$  T exposure). Quantifications of cells exhibiting this dispersed phenotype, showed a >40% and >60% increase in Fam91a1 and WDR11

knock-downs versus shCtr in fixed and live antibody incubation conditions, respectively (Fig. 4c,d).

This phenotype is reminiscent of a retromer-depleted phenotype<sup>69,70</sup>, and suggests a defect in retrograde trafficking of the CI-M6Pr, which could lead to an increased degradation of CI-M6Pr.

Similar to other vesicular transport pathways, retrograde transport from endosomes is greatly intertwined with TGN integrity<sup>30,71</sup>. We therefore tested if and how the TGN might also be compromised by absence of the Fam91a1 and WDR11. For this, we immunostained two independent Fam91a1 knock-down cell lines (#6 and #8), WDR11 knock-down cells and Vps53 knock-down HeLa cells as a positive control for TGN destabilization by GARP complex depletion<sup>40,53,72,73</sup>, with antibodies against the TGN marker protein TGN46. Microscopy images showed a significant decrease in signal intensity of TGN46, when exposure was kept the same for all conditions (Fig. 5a). Both Fam91a1 and WDR11 knock-downs display a similarly reduced TGN46 signal phenotype as the positive control shVps53. Conjointly, they also show a dispersed, vesicular localization of the remaining TGN46 indicating that TGN46 goes from an aggregated juxtannuclear position in control HeLa cells to a scattered small vesicle morphology in the knock-down conditions (Fig. 5b). Quantification of the number of cells displaying the dispersed phenotype show a statistically significant increase of approximately 35% to 40% relative to control (Fig. 5c).

Moreover, we performed a western blot analysis of whole cell lysates of Fam91a1 and WDR11 knock-down cell lines which confirmed the reduced levels of TGN46 seen in the immunostainings (Fig. 5d). We speculate that this decrease might be due to an increased turnover rate of the protein in the absence of our trimeric complex.

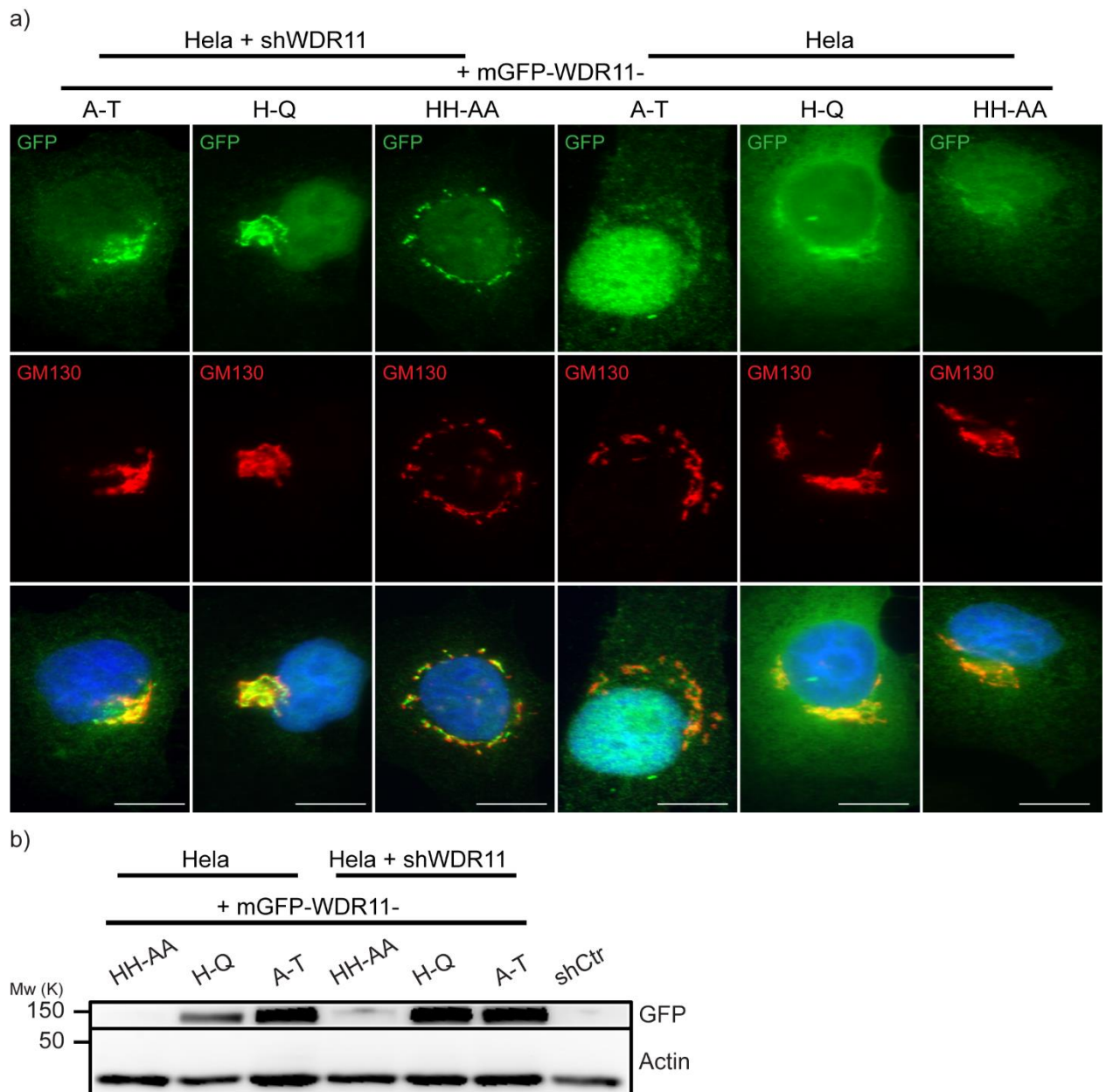


**Figure 3** A-T and H-Q GFP-WDR11 variants localize to the Golgi. **(a)** HeLa WT cells and WDR11 knock-down cells were transfected with one of three different GFP-WDR11 mutated rescue constructs (A-T), (H-Q) and (HH-AA), fixed and immunostained with antibodies against anti-GM130 (red) for cis-Golgi staining, anti-GFP (green) for the ectopically expressed WDR11 fusion protein expression. Nuclei were counterstained with DAPI (blue). **(b)** Western blot of HeLa WT and WDR11-depleted cells expressing the three mutated GFP-WDR11 rescue constructs, blotted against GFP and actin as a loading control. Scale bars, 100  $\mu$ m.

### **3. Protein synthesis inhibition by cycloheximide shows increased degradation of TGN46 in Fam91a1 and WDR11 KD HeLa cells**

Our previous imaging and western-blotting results showed a reduction in TGN46 levels when Fam91a1 and WDR11 are absent. To assess a possible cause, we investigated whether the knock-down of members of the trimeric complex leads to increased proteolytic degradation. We treated shCtr, shFam91a1 and shWDR11 HeLa cells under starving conditions with Cycloheximide (CHX) (20  $\mu\text{g/ml}$ ), a protein synthesis inhibitor, for 3 and 8 hours' time-points, followed by cell lysis and western blot analysis (Fig. 6a). By inhibiting protein synthesis, we can determine whether TGN46 is being more rapidly degraded in the knock-down cell lines or if the different protein levels are the result of altered mRNA levels.

In this representative experiment we observed a decrease in TGN46 levels after the 8h incubation with CHX for all the conditions (Fig. 6a). After normalization to  $\alpha$ -Tubulin, we observed a continuous steeper decline of TGN46 protein levels in shFam91a1 cells, but not in shCtr and shWDR11 (Fig. 6b). In this experiment, shWDR11 degradation rate did not behave as expected, because after 3h of incubation TGN46 levels were higher than the 0h time-point and only decreased 8h after treatment (Fig. 6b). Afterwards, we plotted the degradation kinetics of TGN46 relative to 0h amount of each condition in  $n=3$  independent experiments. Even though not statistically significant, we observed a trend in shFam9a1 and shWDR11 of increased degradation kinetics of TGN46, between time-points 0 and 3h, relative to control.

Surprisingly, shCtr and shWDR11 registered increased TGN46 levels at the 8h time-point, contrary to what was expected, most likely due to low concentration of CHX (Fig. 6c).

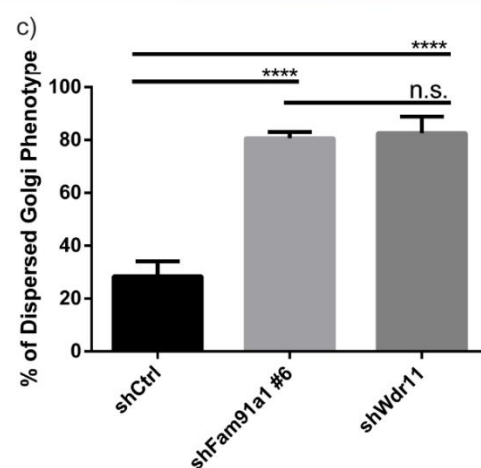
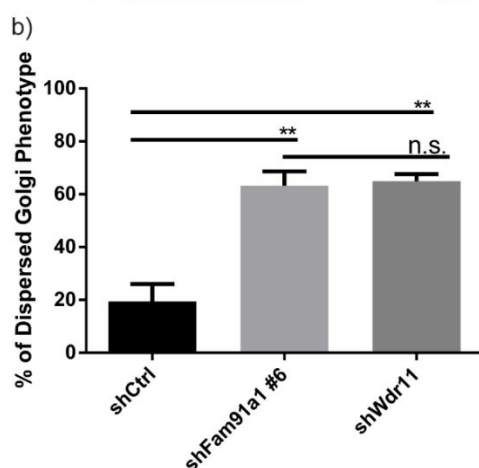
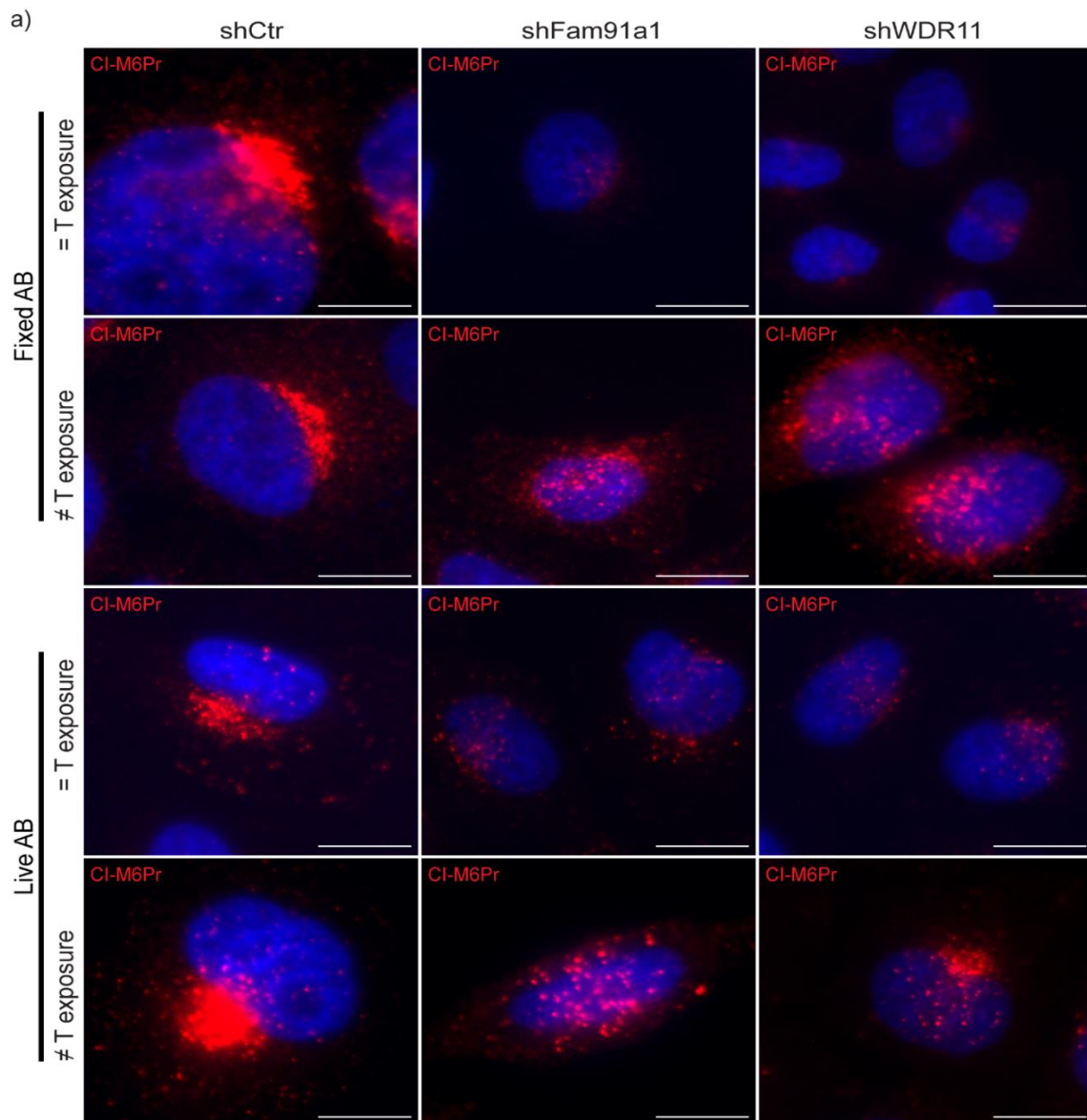


**Figure 4** Impaired retrograde CI-MP6r trafficking in Fam91a1 and WDR11 knock-down cells **(a)** HeLa cells stably expressing shCtr, shFam91a1 or WDR11 were either incubated with CI-MP6r antibody (red) after PFA fixation (**Fixed AB**) or incubated in living cells for 1h at 37°C before fixation (**Live AB**). Cells were either with a fixed exposure time (**= T exposure**) or changed arbitrarily (**≠ T exposure**). Nuclei were counterstained with DAPI (blue). **(b,c)** Quantification of the number of cells displaying a dispersed CI-M6Pr

localization phenotype, versus the condensed phenotype predominant in control cells, in **Fixed AB** incubation **(b)** or **Live AB** incubation **(c)** Means  $\pm$  s.e.m., Live AB incubation,  $n > 50$  cells per condition, 1 representative of  $n = 4$  independent experiments for each condition; Fixed AB incubation,  $n > 50$  cells per condition, 1 representative of  $n = 3$  independent experiments for each condition. \*\*  $P < 0.01$ , \*\*\*  $P < 0.001$ ; \*\*\*\*  $P < 0.0001$ ; n.s., not significant. 1-way ANOVA statistical test. Scale bars, 100  $\mu$ m.

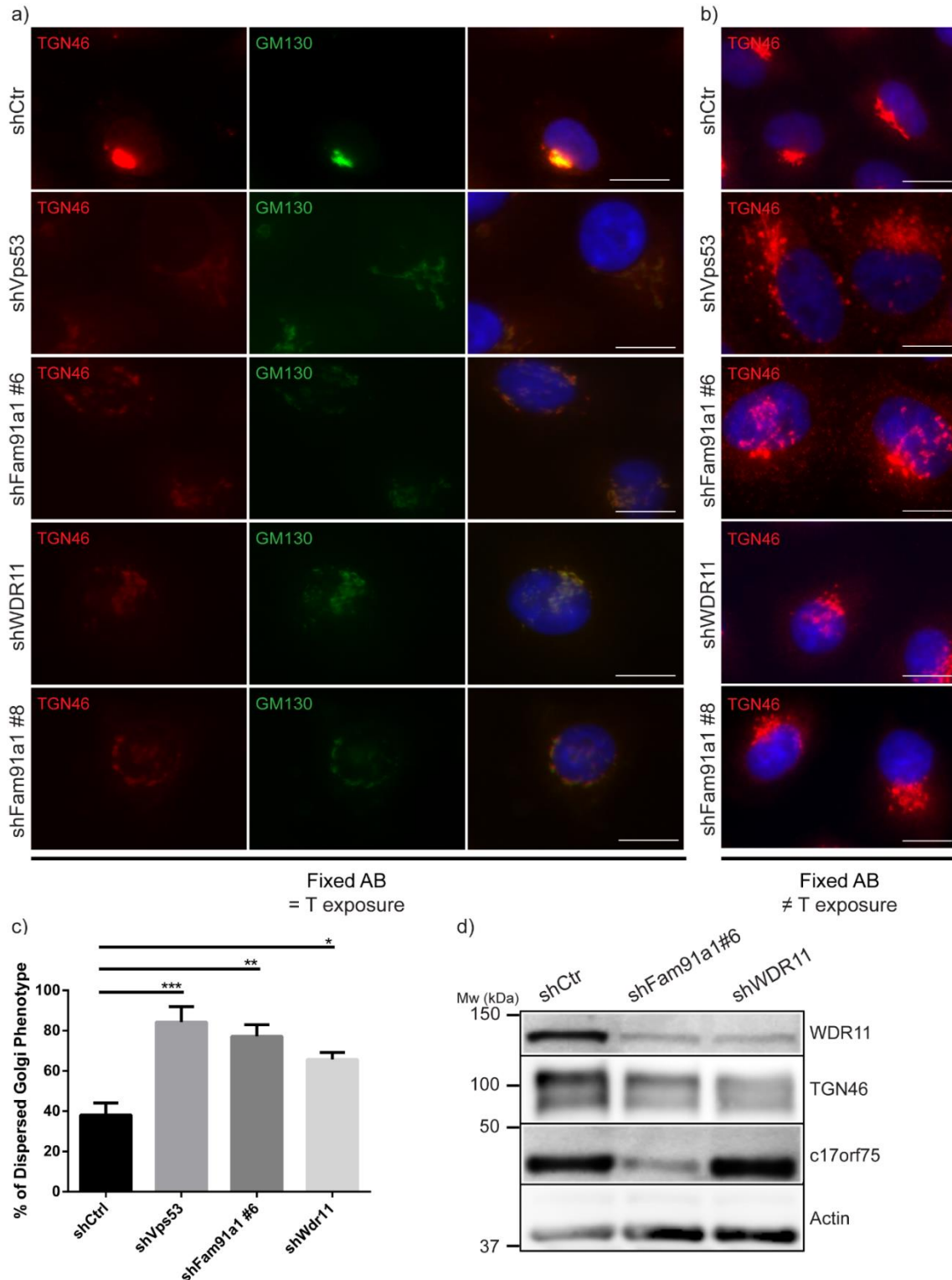


**Figure 5** Fam91a1 and WDR11 knock-down reduce TGN46 protein levels and cause an altered intracellular TGN46 localization similar to interfering with the GARP complex absence condition. **(a,b)** HeLa cells stably

expressing shCtr, shVps53 (GARP complex subunit as positive control), two constructs of shFam91a1 or WDR11 were fixed and immunostained with antibodies against the cis-Golgi marker GM130 (green) and TGN46 antibody (red). Cells were either imaged maintaining the same time of exposure (= **T exposure**) (a) or changed arbitrarily ( $\neq$  **T exposure**) (b). Nuclei were counterstained with DAPI (blue). (c) Quantification of the number of cells displaying a dispersed TGN46 localization phenotype in the indicated cell lines. Means  $\pm$  s.e.m.,  $n > 50$  cells per condition, 1 representative of  $n = 4$  independent experiments for each condition. \*  $P < 0.05$ , \*\*  $P < 0.01$ ; \*\*\*  $P < 0.001$ . 1-way ANOVA statistical test. Scale bars, 100  $\mu\text{m}$ . (d) Reduced TGN46 protein levels in Fam91a1 and WDR11 knock-down cells determined by western blot analysis.

#### **4. Cellular migration and directionality are compromised as $\alpha\beta 1$ integrins are misrouted from FAs at the plasma membrane**

Having established the importance of the trimeric complex in the TGN and in retrograde transport, we investigated whether this complex might play a role for integrin trafficking as it was reported that integrins undergo retrograde transport<sup>49</sup>. We first looked at intracellular, vesicular distribution of  $\beta 1$  integrin in GARP and EARP knockdown cells (Vps53, Vps54 or Syndetin (Vps54 homolog in the EARP complex<sup>45</sup>) siRNA knock-downs) in  $\beta 1$  flox fibroblasts which, showed a severely effect in  $\beta 1$  integrin cytoplasmic localization. Vps53 depleted cells, a core protein member of both GARP<sup>73</sup> and EARP<sup>45</sup> complexes used here as positive control, show a strong vesicle-like distribution of  $\beta 1$  integrins across the cytoplasm which was not apparent in control siRNA transfected cells (Fig. 7a: siVps53).

In siVps54 knock-down fibroblasts we also observed vesicle-like structures positive for  $\beta 1$  integrin in a perinuclear region. Furthermore, some focal-adhesion-like complexes positive for  $\beta 1$  integrin were irregularly distributed through the cell (Fig. 7a: Vps54), leading to a possible impairment of the migration process. In the Syndetin knock-down cells,  $\beta 1$  integrin was more abundant in focal-adhesion-like structures, albeit some vesicles were still present (Fig. 7a: siSyndetin). In parallel we performed a western blot analysis to confirm the Vps53, Vps54 and Syndetin knock-down efficiencies in  $\beta 1$  flox fibroblasts (Fig. 7b). It also confirmed, the correlation between GARP and EARP complexes, since Vps53, Vps54 and to a less extent Syndetin, were reduced in a Vps53 knock-down condition, because Vps53 is a common subunit in both GARP and EARP complexes. The Vps54 knock-down was the least efficient, since when compared to siVps53 and siSyndetin the downregulation was equal, even though a significant decrease was registered in comparison to siCtr.



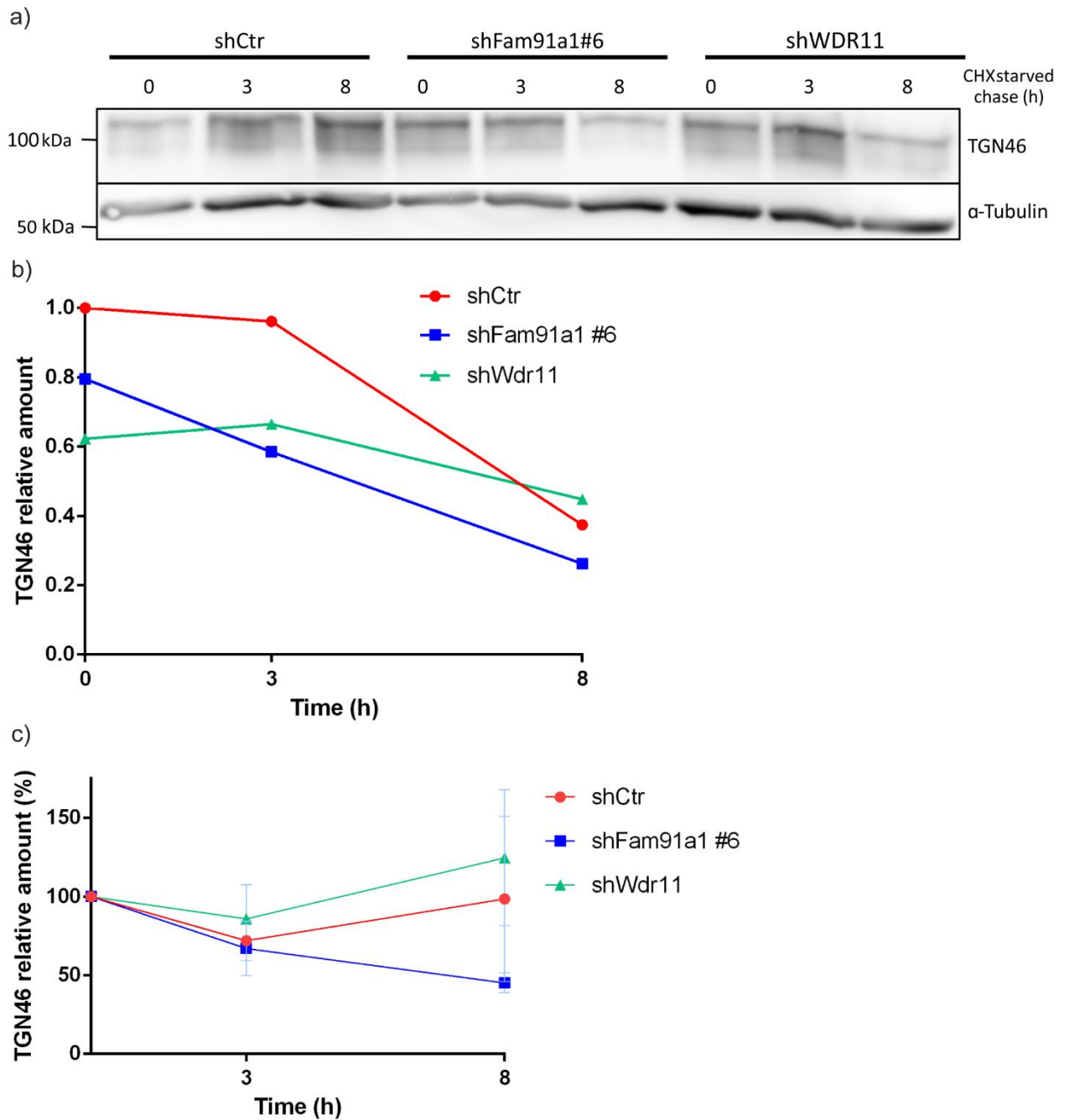


**Figure 6** Cycloheximide chase Fam91a1 and WDR11 knock-down cells suggest increased degradation kinetics of TGN46. **(a)** Western blot analysis of shCtr, shFam91a1 and shWDR11 HeLa cells lysates immunoblotted against TGN46, after Cycloheximide treatment and chased for 8h.  $\alpha$ -Tubulin was used as a loading control. **(b)** Quantification of TGN46 stability in the indicated cell lines normalized to  $\alpha$ -tubulin loading and the shCtr 0h time-point. **(c)** Quantification of TGN46 degradation kinetics in shCtr, shFam91a1 and shWDR11 after Cycloheximide treatment (20  $\mu$ g/ml) followed by chase for 8 hours. Means  $\pm$  s.e.m., Time (h), hours.  $n=3$  independent experiments for each condition.

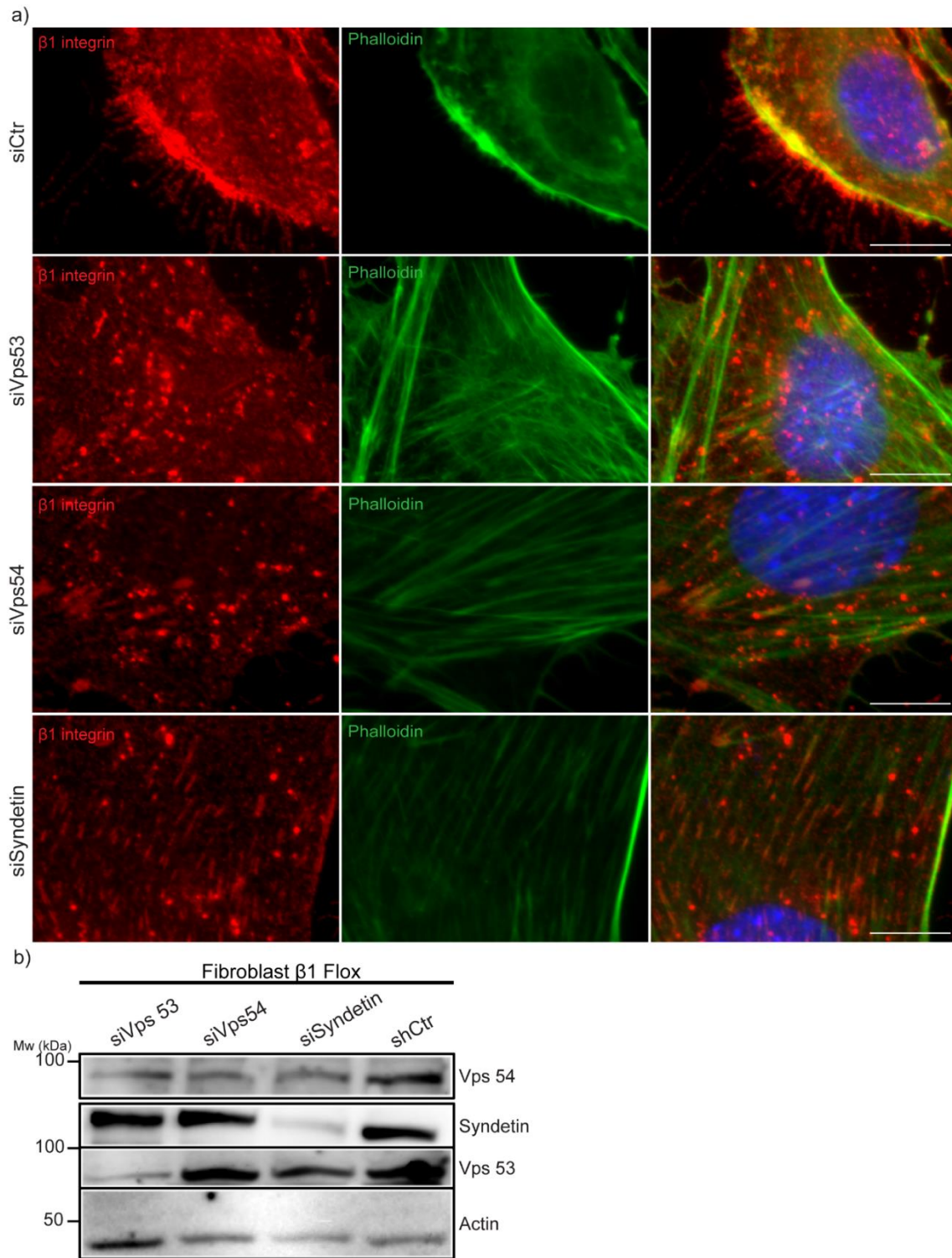


**Figure 7** siRNA-mediated depletion of GARP and EARP subunits interfere with  $\beta 1$  integrin trafficking and recycling back. **(a)**  $\beta 1$  flox fibroblasts transiently transfected with siRNAs against Vps53, Vps54 (GARP-specific subunit) and Syndetin (EARP-specific subunit) were fixed and stained with antibodies against  $\beta 1$  integrin antibody (red) and Phalloidin to visualize F-Actin marker (green). Cells were imaged in a fluorescence microscopy. Nuclei were counterstained with DAPI (blue). Scale bars, 100  $\mu$ m. **(b)** Western blot analysis of the indicated siRNA-transfected  $\beta 1$  flox fibroblasts to determine the knock-down efficiency. Actin was used as a loading control.

This means, either Vps54 presence is also affected by Vps53 and Syndetin or the siRNA silencing was not completely efficient for Vps54 (Fig. 7b). The knock-down of Syndetin also caused a moderate decrease in Vps53 protein when compared to the control, suggesting a relation between Vps53 and Syndetin and not between Vps54, since knock-down of the latter did not affect Vps53.

Overall, these results suggest a relation between the integrin trafficking and the functionality of TGN and endosomes.

To investigate the involvement of the trimeric complex in the integrin trafficking, we performed  $\alpha 5$  and  $\beta 1$  integrin immunostainings in Fam91a1 and WDR11 knock-down HeLa cells. As expected, in control cells the integrin heterodimer localized to focal-adhesion complexes at the plasma membrane (Fig. 8a,b: shCtr); while in Fam91a1 and WDR11 knock-down cells,  $\alpha 5$  and  $\beta 1$  integrin were mostly localized in scattered cytoplasmic structures, particularly evident in a juxtannuclear position reminding of the Golgi complex (Fig. 8a,b: shFam91a1/WDR11).

Collectively, these results suggest an involvement of the Fam91a1/WDR11/C17orf75 in the trafficking of  $\alpha 5\beta 1$  integrins.

$\alpha 5\beta 1$  integrin is a major player in cell adhesion and migration and its precise subcellular localization and trafficking is crucial for cell motility. Therefore, we tested for a direct connection between the Fam91a1/WDR11/C17orf75 complex and cell migration. We performed wound healing assays on confluent shCtr, shFam91a1 #6, shWDR11, shFam91a1 #8 and GFP-Fam91a1 (rescue construct) HeLa cells, in starving condition after treating the cells with mitomycin C, a cell division inhibitor (Fig. 9a-10a). We recorded the cell migration by time lapse microscopy and quantified the cell migration with respect to single-cell velocity and directionality. Images of three representative time-points (0, 12 and 24h) for each cell lines were displayed, showing how cells collectively migrated.

The shFam91a1 #6, shFam91a1 #8, shWDR11 and the GFP-Fam91a1 rescue cell lines displayed reduced wound area closure (Fig. 9a-10a) as well as a reduced single-cell migration velocity (Fig. 9b-10b). Pointing out that either Fam91a1 or WDR11 knock-

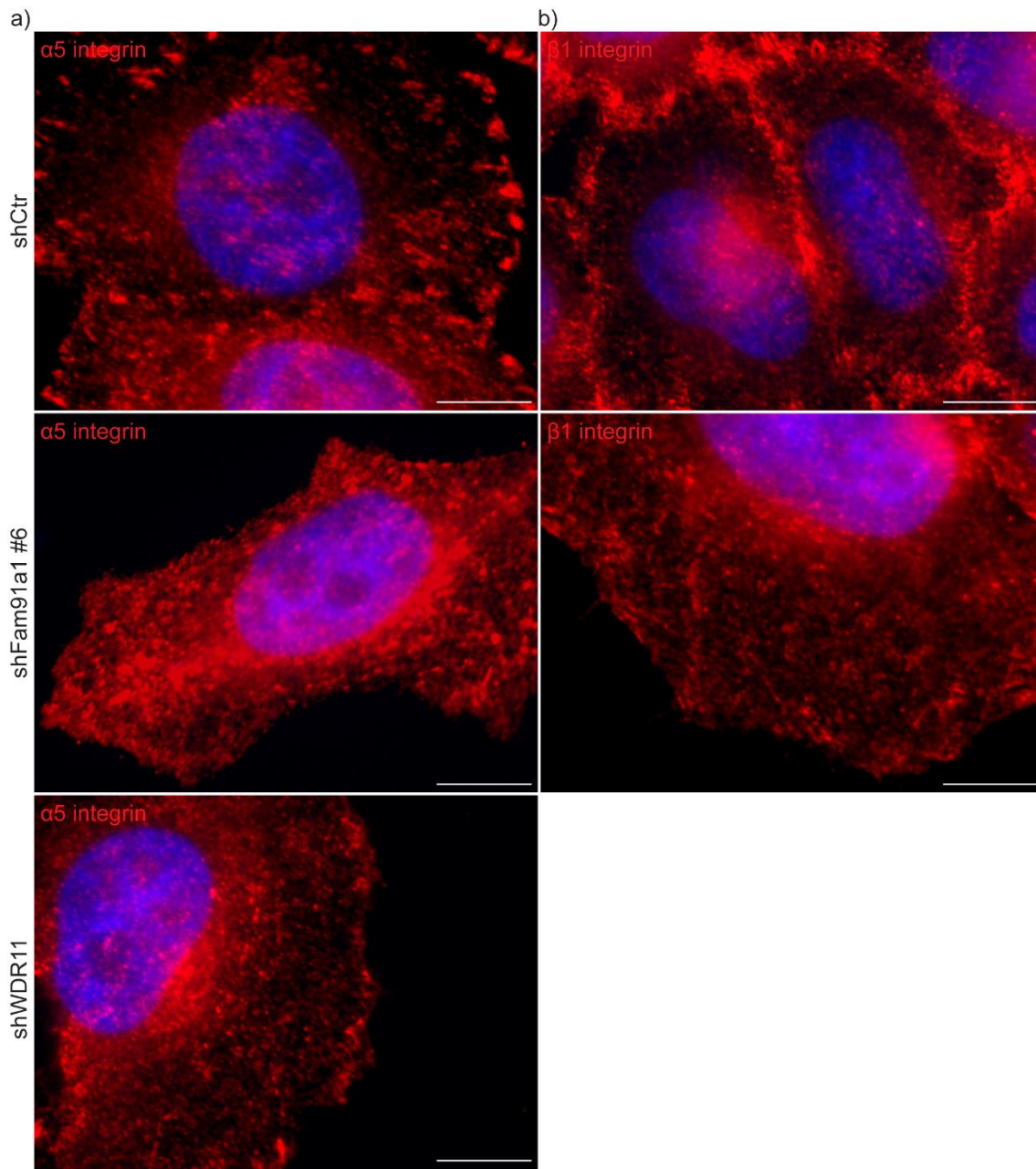


**Figure 8** Fam91a1 and WDR11 knock-downs interfere with proper  $\alpha 5$  integrin trafficking. **(a)** HeLa cells expressing shCtr, shFam91a1 or shWDR11 were fixed and incubated with an  $\alpha 5$  integrin antibody (red), followed by fluorescence microscopy imaging. Nuclei were counterstained with DAPI (blue). Scale bars, 100  $\mu\text{m}$ .

down was sufficient to partially disrupt cell migration. We also observed an increase in the directionality or also called path persistence (ratio of the effective maximum displacement to the actual trajectory length)<sup>49</sup>, in cells depleted of Fam91a1 or WDR11 (Fig. 9c-10c). We did not observe a rescue of cell migration when GFP-Fam91a1 was re-expressed in Fam91a1 knock-down cell lines indicating that the GFP tag likely interferes with some of the Fam91a1 functions. Together these results establish a direct

relationship between our Fam91a1, WDR11 and C17orf75 trimeric complex and its role on the speed and randomness of cell migration.

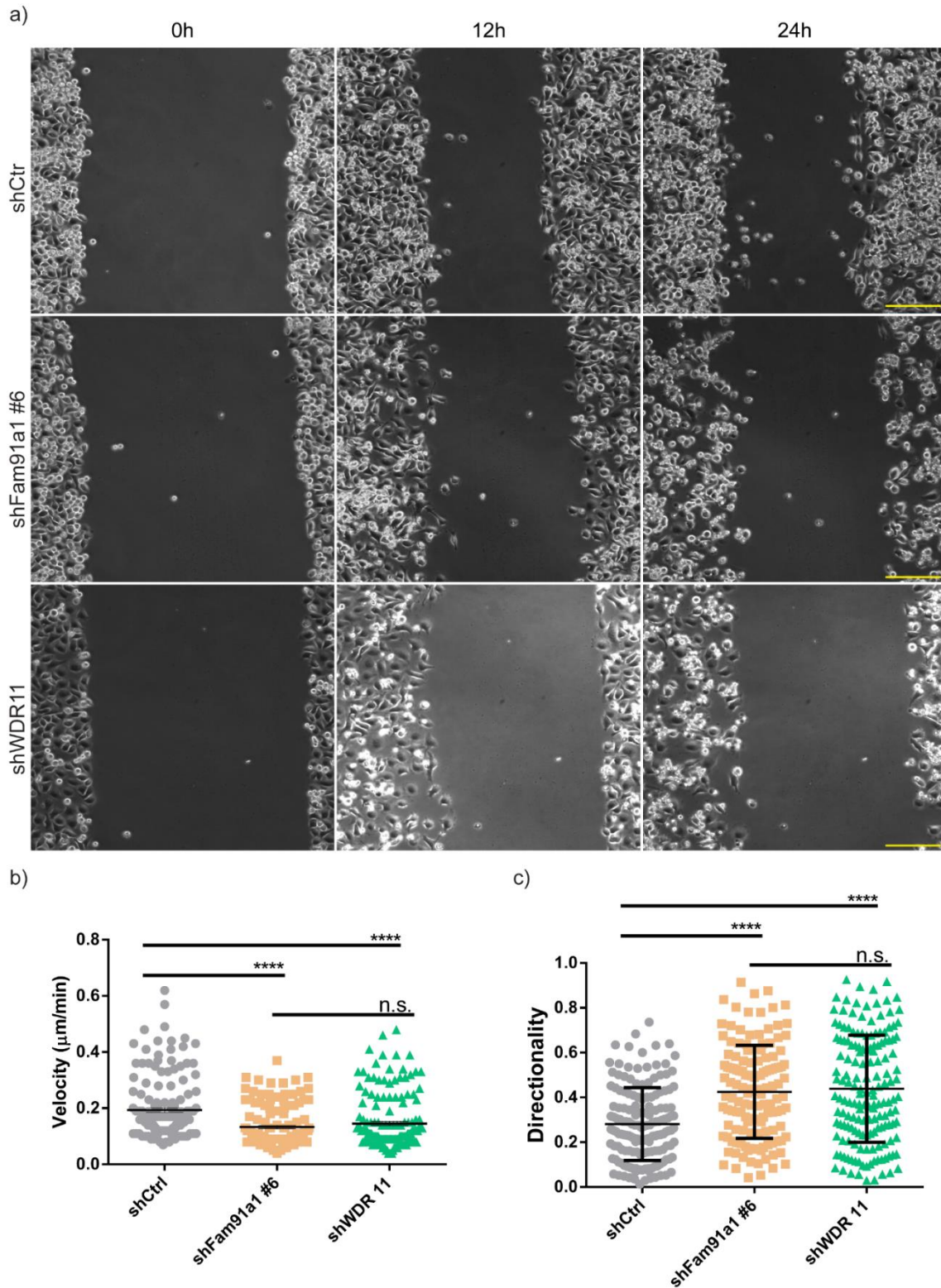


**Figure 9** Fam91a1 and WDR11 depletion impairs cell migration. **(a)** HeLa cells stably expressing shFam91a1 and shWDR11 were seeded overnight under starving conditions on fibronectin coated surfaces, followed by Mitomycin C treatment (25  $\mu\text{g}/\text{ml}$ ) for 2 hours and a wound scratch across the confluent dish. Cells were imaged at 37°C by live cell microscopy for 24 hours. **(b,c)** Quantification of cell velocity ( $\mu\text{m}/\text{min}$ ) **(b)**

and directionality (c) in the wound healing assay. Means  $\pm$  s.e.m.,  $n > 50$  cells per condition, 1 representative of  $n = 3$  independent experiments for each condition. \*  $P < 0.05$ , \*\*  $P < 0.01$ ; \*\*\*  $P < 0.001$ , \*\*\*\*  $P < 0.0001$ ; n.s., not significant. 1-way ANOVA statistical test. Scale bars, 3mm.

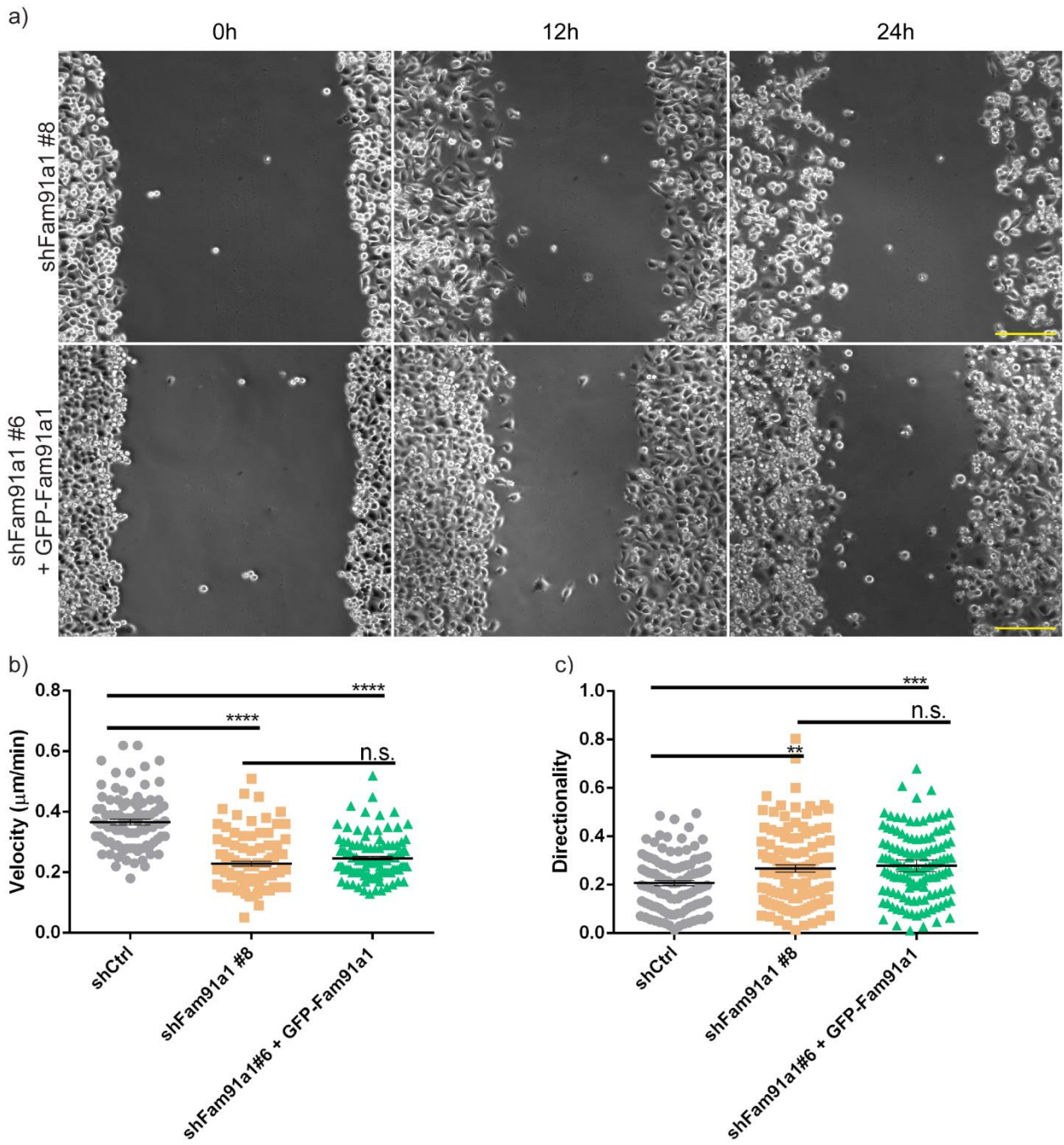


**Figure 10** GFP-Fam91a1 re-expression in Fam91a1 depletion HeLa cells does not fully rescue the shFam91a1 migration defect. **(a)** HeLa cells stably expressing shFam91a1 #8 and the shFam91a1 #6 + GFP-Fam91a1 constructs were seeded on fibronectin-coated surfaces overnight under starving conditions, followed by Mitomycin C treatment (25  $\mu\text{g}/\text{ml}$ ) for 2 hours and a by a wound scratch across the confluent dish. Cells were imaged at 37°C by live cell microscopy for 24 hours. **(b,c)** Quantification of cell velocity ( $\mu\text{m}/\text{min}$ ) **(b)** and directionality **(c)** in the wound healing assay. Means  $\pm$  s.e.m.,  $n > 50$  cells per condition, 1 representative of  $n = 3$  independent experiments for each condition. \*  $P < 0.05$ , \*\*  $P < 0.01$ ; \*\*\*  $P < 0.001$ ; \*\*\*\*  $P < 0.0001$ ; n.s., not significant. 1-way ANOVA statistical test. Scale bars, 3mm.

## **5. Proteomic Mass-Spectrometry screening analysis of knock-downs and Biotin pull-downs of the trimeric complex proteins**

In order to identify potential proteins interactors or regulators of the Fam91a1, WDR11, C17orf75 complex and to determine pathways regulated by this complex a whole-proteome mass-spectrometry (MS) screening of control HeLa cells and cells depleted of Fam91a1 and WDR11 and was performed.

Firstly, we confirmed the knock-down efficiency of the different cells lines by western blot analysis, which confirmed the efficiency of the protein expression silencing (Fig. 11a). For the whole-proteome analysis  $5 \times 10^6$  cells of the three cell lines were lysed and each condition analyzed in triplicates. The MS screening was carried out in the MPI of Biochemistry mass spec core facility and the unfiltered results were analyzed with the Perseus to highlight the statistically relevant changes in protein expression between shFam91a1, shWDR11 and control. This filtering resulted in 1326 proteins with statistically relevant deregulated expression out of 8159 initially found. Perseus software allowed us to do a cluster heat map illustrating that the Fam91a1 deficiency is responsible for the larger number of protein expression variations between Fam91a1 and WDR11 compared to shCtr (Fig. 11b). As a positive control for the experiment we looked into both Fam91a1 and WDR11 expression profiles throughout the three replicates of each of the three conditions. Since these proteins behaved as expected (WDR11 downregulated in both knock-down conditions; Fam91a1 just on its knock-down condition) more confidence can be attributed to the remaining results. (Fig. 11c,d).

Then, to find and characterize the body of altered proteins that constituted each knock-down, we first set the knock-down expression profile as the reference to all other proteins who might have a similar expression profile. Then, we searched for a number of proteins that showed a similar profile, until an arbitrarily attributed signal-to-noise ratio was reached, comparing the sum of the expression profiles of the unknown

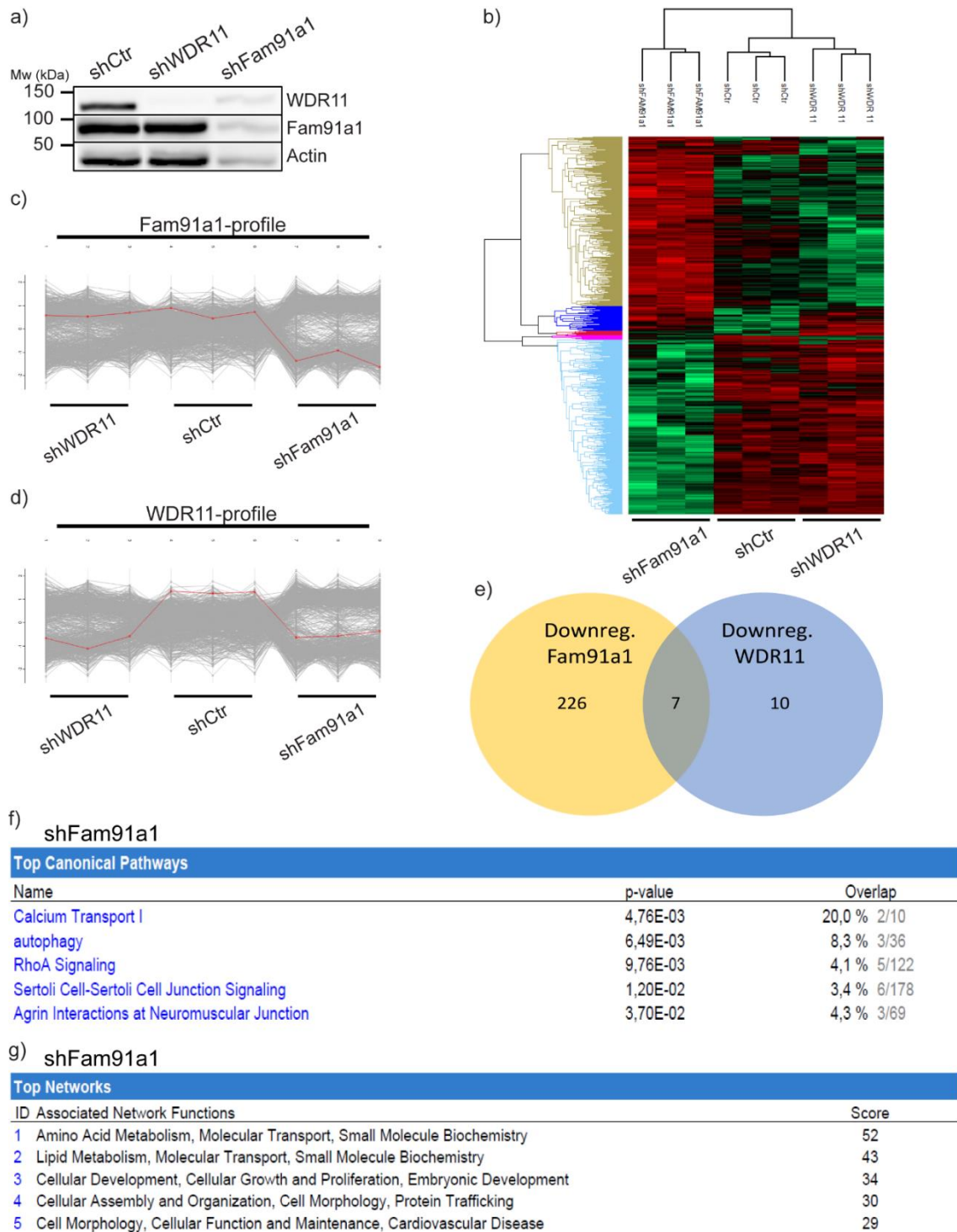


**Figure 11** Whole Proteome Mass-Spectrometry on control and Fam91a1 and WDR11-depleted HeLa cell lines. **(a)** Western blot analysis of shCtr, shFam91a1 and shWDR11 HeLa cell lines confirms the protein knock-down. **(b)** Cluster analysis representation of whole-proteome MS results ( $n=5$  clusters). **(c,d)** Protein expression profile in all cell lines replicate's of Fam91a1 **(c)** and WDR11 **(d)**. **(e)** Number of proteins displaying a similar expression profile to Fam91a1 and/or WDR11.  $n=3$  replicates; 1-way ANOVA statistical test, permutation-based FDR=0.05;  $S_0=0.05$ . Z-score normalization. **(f,g)** Qiagen's Ingenuity Pathway Analysis (IPA) data mining software analysis of the most statistically significant downregulated protein expression of Fam91a1 KD in categorical groups of Canonical Pathways **(f)** and Networks **(g)**

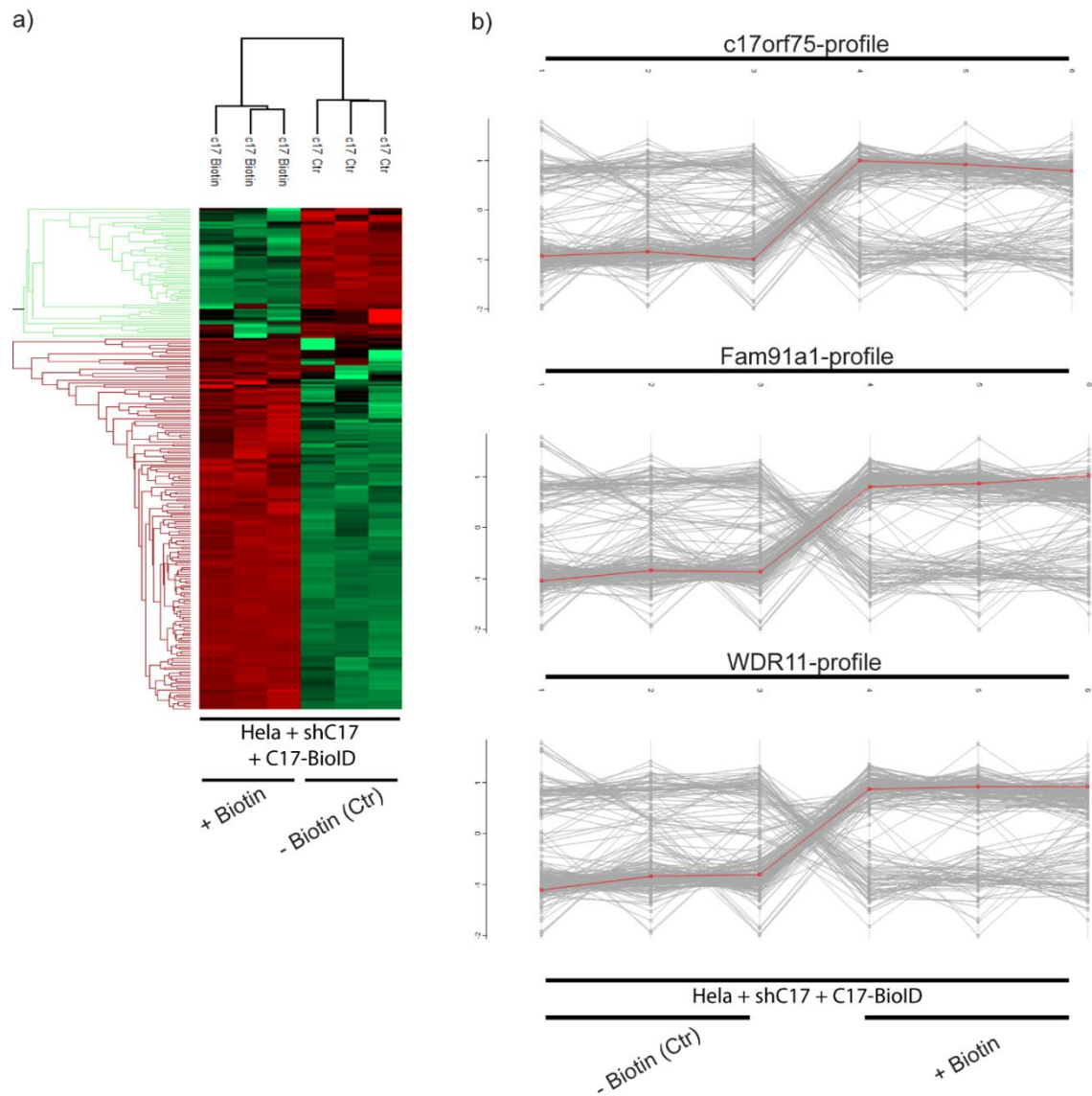


proteins and the similarities to the downregulated proteins in the knock-down (shFam91a1/shWDR11) original expression profile. We registered only 7 proteins commonly downregulated in both knock-downs, from a pool of 226 with a downregulated in Fam91a1 knock-down profile and a pool of 10 with a downregulated in WDR11 knock-down profile (Fig. 11e).

Among the seven downregulated proteins, in both knockdown cell lines, were Perilipin 2 (PLIN2), ceramide synthase 1 (CERS1), desaturase-sphingolipid 1 (DEGS1), autophagy-related protein 12 (ATG12), vacuolar protein sorting 13 (Vps13), which are associated with spermatogenesis, germ cell differentiation or autophagy<sup>60,74</sup>.

In order to analyze the 226 proteins downregulated in shFam91a1 cells, we used Qiagen's Ingenuity Pathway Analysis® (IPA) data-mining software, which grouped the proteins according to different categories based on different criteria, such as canonical pathways involved, networks diseases, etc. We categorized the list of proteins significantly downregulated in Fam91a1-depleted HeLa cells, because it was the condition which showed most changes compared to control HeLa cells. We found proteins involved in the canonical pathways of Sertoli-cell junction signaling, RhoA signaling and autophagy (Fig. 11f). Interestingly, the literature showed a relevant connection between retrograde transport machinery (Golgi-to-ER) and autophagy regulation and function (autophagy regulators trafficking)<sup>75</sup>. In our MS screening we found, Beclin-1 (BECN1), Autophagy related 9A (ATG9A), both associated with autophagy and Vacuolar protein sorting 18 (Vps18), a member of endosomal tethering complexes, to be downregulated in Fam91a1 knock-down. Through another categorization of the IPA analysis, we found different altered networks in Fam91a1 knock-down, which confirmed the importance of the trimeric complex in the molecular transport, protein trafficking, cellular growth and proliferation, lipid metabolism (autophagy-related) and cell morphology (Fig. 11g).

In addition to the whole proteome analysis, interactome analysis of WDR11 and C17orf75 was performed in the department. For this, streptavidin pull-downs of C17orf75-BioID and WDR11-BioID expressing HeLa cells were carried out after incubating the cells overnight in the absence and presence of 50  $\mu$ M biotin (Fig. 12-13). When cells were supplied with an excess of biotin, in both pull-down experiments a



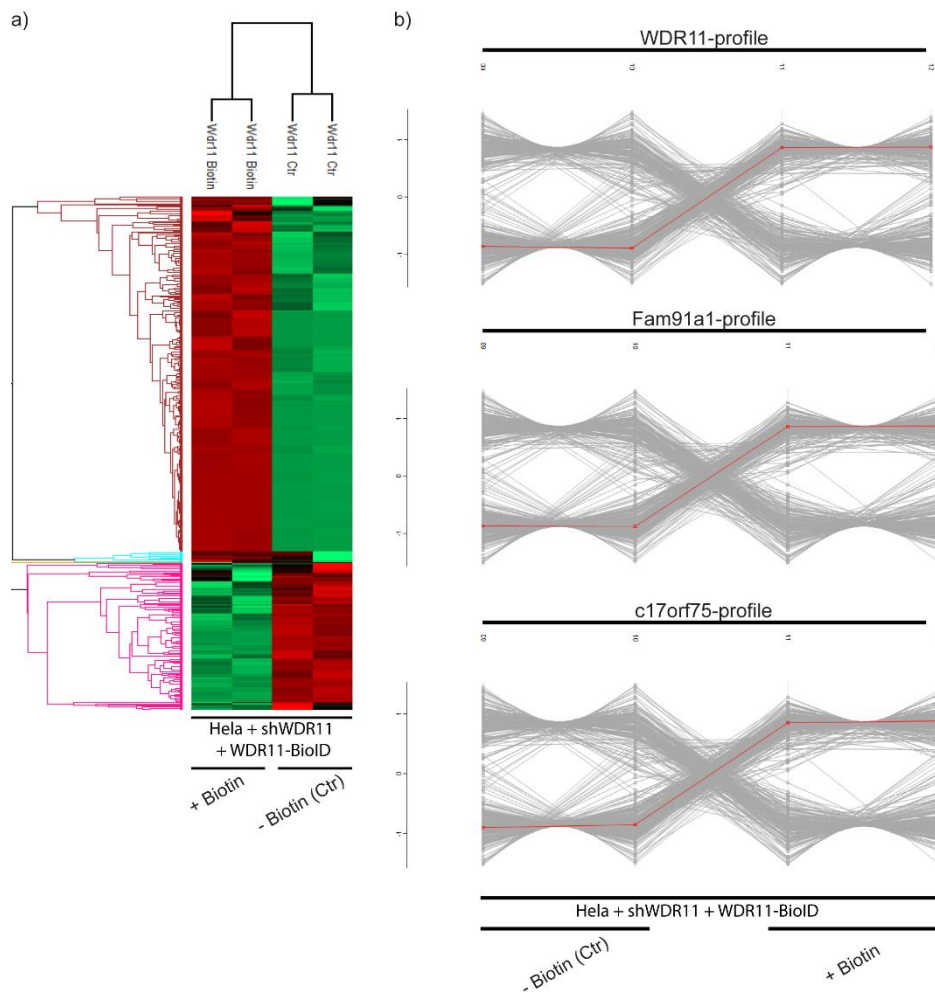


**Figure 13** Mass-Spectrometry analysis of the WDR11 interactome by WDR11-BioID **(a)** Cluster analysis representation of interactome MS results ( $n=3$  clusters) of HeLa + shWDR11 + WDR11-BioID cells pull-down in the absence or presence of 50  $\mu\text{M}$  Biotin.  $n=2$  replicates; 1-way ANOVA statistical test, permutation-based FDR=0.05;  $S_0=0.05$ . Z-score normalization. **(b)** Protein expression profile in all cell line's replicates of WDR11, Fam91a1 and C17orf75.

paramount change in the number of proteins baited was attained. The experiments were carried out in replicates.

As expected Fam91a1, WDR11 and C17orf75 were highly enriched in pulldown samples after biotin treatment, thus validating the experiment (Fig. 12b-13b). Finally, the significant proteins found in the biotin pull-down were clustered, for the WDR11-BioID the filtering and statistical analysis resulted in 640 altered proteins expression out of 790 initially found. For the C17orf75-BioID pull-down the filtering and statistical analysis resulted in 220 expression proteins altered proteins expression out of 615 (Fig. 12a-13a).

Proteins identified in both (the C17orf75 and WDR11) interactomes were proteins from WASH complex subunits and related to Golgi apparatus, small GTP-binding family and gonadal and gametes development. In an individual context, C17orf75 biotin pull downs showed some interesting proteins, such as ATG9, CI-M6Pr, Talin and Perilipin4. Whereas for WDR11 biotin pull downs, we found Vps complex subunits: Vps53, 52, 51, 33b and 45; Integrin-linked protein kinase (Ilk) and Rab11 interacting protein.

Altogether, these data suggest the importance of the trimeric complex for the regulation of cellular pathways and help to identify potential novel interactors which could shed light onto the molecular mechanism of Fam91a1, WDR11, C17orf75 complex function.



# Discussion



This thesis work focused on the characterization of three poorly studied proteins, Fam91a1, WDR11 and C17orf75, and their involvement in integrin trafficking. Most of the studies that have been published, are about the WDR11 protein, a member of the highly diverse WD repeat family of proteins, which are responsible for coordinating multiprotein complexes<sup>31,76</sup>. WDR11 in particular, has been mostly known to bind transcription factor EMX1, in the context of idiopathic hypogonadotropic hypogonadism (IHH) disease and Kallman's syndrome (KS)<sup>67</sup>. Another study characterized WDR11 as a major key factor in promoting Herpes Simplex Virus (HSV) viral yields by interaction with its virion components at the trans-Golgi network<sup>31</sup>. Other interactors of WDR11 were reported, however, further studies are required to shed light on the biological significance of the WDR11 interactions.

Fam91a1 and C17orf75 are two poorly characterized proteins; Fam91a1 and WDR11 were reported to interact with dysbindin, a synapse-enriched schizophrenia-associated protein<sup>64</sup> and C17orf75 was shown to bind Wdr11 and being required to sensitize cells to ricin toxin<sup>33</sup>.

Herein we demonstrate novel interactions between Fam91a1, WDR11 and C17orf75 that form a trimeric complex at the Golgi apparatus and are involved in retrograde trafficking and cell migration. In HeLa cells, loss of FAM91a1 results in a major loss of WDR11 and C17orf75 protein levels while knock-down of WDR11 had not effect on Fam91a1 and C17orf75 indicating that the stability of the trimeric complex is Fam91a1-dependent.

Point mutations in *WDR11* gene, present on the human chromosome 10q26, were identified in male patients with IHH (idiopathic hypogonadotropic hypogonadism) disease and Kallman's syndrome<sup>67</sup>. We showed that expression of these WDR11 versions (A435T; H690Q; HH507/513AA) in WDR11 knock-down HeLa cells resulted in no observable change in the Golgi morphology and WDR11 localization which suggests that these mutations, even though they have a been found in defective puberty development and endocrine homeostasis of sex hormones<sup>77</sup>, they are not decisive for the integrity and cellular localization of WDR11 or the Golgi apparatus in HeLa cells.

Adding to that, WDR11 was also found residing in the trans-Golgi network (TGN)<sup>31</sup> and interacting with the autophagy-related protein ATG8<sup>61</sup> which localizes in the



ER-Golgi vicinity<sup>78-81</sup>. Thus, we deemed relevant to further study how the trans-Golgi network might be affected in the absence of the trimeric complex.

The trans-Golgi network is an important coordinating hub in several transport routes within the cell, such as in the secretory, retrograde, recycling or endocytic pathways<sup>30,47,82,83</sup>. We directed our focus to the retrograde trafficking route function of the trans-Golgi network and could demonstrate that this function is compromised in the absence of Fam91a1 or WDR11. The trafficking of the cation-independent mannose 6-phosphate receptor (CI-MP6r), an acid hydrolase receptor and one of the most studied retrograde transport cargo proteins, is impaired in the absence of the trimeric complex. We observed reduced protein levels and an up-to-60% increase in a scattered vesicle phenotype of CI-M6Pr similar to what has been observed in cells depleted of the retromer complex<sup>69,70</sup>. This complex responsible for binding the cytosolic domain of CI-M6Pr through Vps35, and retrieve the receptors from the early endosomes back to the TGN<sup>84</sup>.

Our hypothesis is that the trimeric complex mediates the retrieval of CI-M6Pr from the endosomes to the trans-Golgi network. A knock-down of Fam91a1 or WDR11 would therefore lead to inefficient endosome-to-TGN retrieval, a scattered CI-M6Pr subcellular localization and possibly an increased degradation of CI-M6Pr, due to an increased transport of the CI-M6Pr to the lysosomes for degradation, similar to the phenotype of the retromer knocked-down<sup>69</sup>. While we observed reduced CI-M6Pr levels indicative for increased lysosomal transport and degradation, no significant change in CI-M6Pr plasma membrane levels was observed, although the early endosomes and plasma membrane trafficking was reported to be an alternative CI-M6Pr trafficking route in retromer-depleted cells<sup>70</sup>.

Another possibility was whether this disrupted localization of CI-M6Pr and its decreased levels might be associated with the human homolog of the yeast Golgi-associated retrograde protein tethering complex (GARP)<sup>47,73</sup>. Depletion of GARP subunits results in inhibition of the retrograde transport of CI-M6Pr from the endosomes to the TGN<sup>40</sup> which then accumulate in endosome-resembling vesicles similar to the phenotype we observed after Fam91a1 or WDR11 knock-down. Even though the majority of the CI-M6Pr signal is dispersed through the cell in the small vesicles, a

partition still seems to aggregate to a juxtannuclear localization, suggesting that other different routes might still be functioning in transporting CI-MP6r to the TGN through other tethering factor complexes like, Rab9-TIP47 or PACS1-AP1<sup>30,85</sup>.

In parallel to CI-M6Pr we examined the behavior of TGN46, another well-characterized cargo of the trans-Golgi network retrograde pathway<sup>86</sup>. Similar to CI-M6Pr, TGN46 also localized to small scattered vesicles when Fam91a1 and WDR11 were knocked-down and the overall protein expression of TGN46 was reduced.

More experiments are needed to describe the role of the Fam91a1, WDR11, C17orf75 complex in retrograde transport and to define the extend of its effect on retrograde transport. For example, one could address if proper sorting of lysosomal hydrolases to the lysosome (ex. Cathepsin D, cargo of CI-MP6r) is still occurring and confirm the degradation rate kinetics of CI-M6Pr in the Fam91a1 and WDR11 knock-down conditions. It would also be beneficial to identify the nature of the CI-M6Pr positive vesicles in the scattered phenotype by co-staining with antibodies against specific marker proteins and to assess if the remaining CI-M6Pr signal in the juxtannuclear position is due to a parallel retrograde trafficking route or if the trimeric complex also plays a role in the exiting of cargoes from the Golgi.

Fam91a1 and WDR11 depleted cells phenotype was very alike to the knock-down of VPS53, a core subunit of the GARP tethering complex<sup>73</sup>. As previously reported, GARP depletion induces the formation of dispersed small vesicles of TGN46<sup>40</sup> that are already past the point of sorting for lysosomal degradation. However, in our experiments TGN46 expression was reduced indicating that sorting for lysosomal degradation is still functioning. These data also indicate that the trimeric complex regulates TGN46 retrograde transport differently from GARP complex. Accordingly, our first cycloheximide chase assays suggested that indeed the trimeric complex absence increases the degradation kinetics of TGN46. Further experiments are needed to explain the mechanistic differences between the function of the trimeric complex and GARP complex in cargoes retrograde transport.

Until recently, the models of integrin trafficking did not consider retrograde trafficking as an intracellular itinerary important for integrin-mediated cellular functions. However, Shafaq-Zadah *et al.* recently shed light onto the role of TGN-

mediated retrograde trafficking of  $\beta 1$  integrin in persistent polarized cell migration<sup>49</sup>. After establishing a functional connection between the Fam91a1/WDR11/C17orf75 trimeric complex and the TGN-associated retrograde transport, we examined  $\alpha 5\beta 1$  integrin subcellular localization in Fam91a1 and WDR11 knock-down HeLa cells. We observed an altered  $\alpha 5\beta 1$  integrin subcellular localization similar to cells depleted for GARP and EARP complexes subunits.

The GARP complex, as mentioned before, is a docking complex at the TGN<sup>53</sup> crucial for endosome-to-Golgi retrieval of proteins, whilst the endosome-associated recycling protein complex (EARP) is a tethering complex in the endocytic recycling pathway that associates with Rab4-positive endosomes from the short-loop recycling pathway<sup>45</sup>. Both complexes share the Ang2, Vps52 and Vps53 subunits<sup>29,45,87</sup>, but GARP also contains Vps54 as the specific subunit, while the EARP complex includes Syndetin. We show that the depletion of core subunits of these two complexes results in a scattered vesicular distribution of  $\beta 1$  integrin opposed to its localization at the focal adhesions in control cells. This might lead to impaired cell migration, as adhesion complexes are needed in the plasma membrane to establish the traction points in which cells migrate<sup>13,88</sup>.

Our results confirm the documented involvement of GARP and EARP complexes in retrograde transport and endosome recycling, respectively, and the role of retrograde trafficking on  $\beta 1$  integrin subcellular localization and transport<sup>49</sup>. These results served as a positive control for the observed scattered vesicle-like subcellular distribution of  $\alpha 5\beta 1$  integrin in the cytosol in Fam91a1- and WDR11-depleted cells. Similar to the GARP and EARP complexes, the Fam91a1/WDR11/C17orf75 complex is responsible for the proper trafficking of  $\alpha 5\beta 1$  integrin to focal adhesions as the interference with Fam91a1 or WDR11 function causes an accumulation of  $\alpha 5\beta 1$  integrin in endosomal vesicles. This further supports the functional association between retrograde trafficking machinery and integrin trafficking routes.

Again, further work is necessary to address the question of how these events, mediated by Fam91a1/WDR11/C17orf75 complex, take place. We speculate that the trimeric complex might play a role at one of the steps of budding, transport, tethering, docking or fusion of the vesicles from the endosomal system to the trans-Golgi network,

as part of the overall process of retrograde trafficking of  $\alpha 5\beta 1$  integrins and other cargo proteins.

Integrins play a central role in cell adhesion and migration<sup>4,22</sup> and require defined distribution, subcellular localization and trafficking to exert their functions. After endocytosis into the endosomal system, the recycling of  $\alpha 5\beta 1$  integrin back to the plasma membrane through the retrograde route is important for persistent cell adhesion and migration of highly polarized cells<sup>49</sup>. Here we have uncovered another subset of proteins, Fam91a1 and WDR11 that regulate random cell migration. When Fam91a1 and WDR11 were depleted in HeLa cells, cell migration speed was significantly reduced while the directionality (also called, path persistence) increased significantly. A GFP-tagged Fam91a1 failed to rescue the cell migration speed and randomness, suggesting that the GFP tag somehow interferes with Fam91a1 function.

Reduced directionality (increased randomness), is characteristic of an impaired retrograde trafficking machinery, such as syntaxin 16 and Rab6<sup>49</sup> while increased directionality (path persistency) and increased migration speed is characteristic of impaired Rab11-mediated long-loop recycling of  $\alpha 5\beta 1$  integrin<sup>89</sup>. Our results suggest that Fam91a1 and WDR11 might play a role in distinct trafficking pathways as it promotes random cell migration contrary to the retrograde trafficking factors syntaxin 16 and Rab6 but on the other hand increases cell migration speed like Rab11-mediated recycling. This might indicate that the Fam91a1/WDR11/C17orf75 complex might be a central pivot in coordinating integrin trafficking events, including the ones involved in Golgi-mediated retrograde trafficking and Rab11-mediated recycling.

To unravel more information about the cellular role(s) of the Fam91a1/WDR11/C17orf75 complex future experiments might include assessments, of integrin distribution at the plasma membrane, cell spreading, cell adhesion or Golgi polarization in wound healing assays in control and Fam91a1 or WDR11-depleted cells.

Our findings prompted us to look for further new interactors and regulators of the Fam91a1/WDR11/C17orf75 complex that might provide us with insights of the extent to which this trimeric complex is regulating other major cellular pathways. Through a whole-proteome mass-spectrometry screening of HeLa cells depleted of either Fam91a1 or WDR11, and an interactome analysis of WDR11- and C17orf75-BioID

pull-downs we were able to identify several novel pathways potentially regulated by one or more proteins of the Fam91a1/WDR11/C17orf75 complex.

By comparing the expression profiles of different proteins we assembled a set of proteins downregulated in either Fam91a1 or WDR11 knock-down cells, and identified seven proteins to be downregulated in both cell lines. These proteins were, Perilipin 2 (PLIN2) a lipid-droplet storage protein that has been involved in spermatogenesis in Sertoli cells<sup>74</sup>; ceramide synthase 1 (CERS1) a protein that promotes autophagy, particularly, phagophore induced mitophagy<sup>90</sup>; desaturase-sphingolipid 1 (DEGS1) another protein involved in autophagy signaling pathway<sup>91</sup>; autophagy-related protein 12 (ATG12) a protein part of one ubiquitin-like conjugated system related to autophagosome maturation<sup>62,92</sup>; and vacuolar protein sorting 13 (Vps13) involved in the regulation of autophagy at different stages<sup>60</sup>. Thus, the proteomic analysis of the cell lines point to autophagy as a common pathway to be intertwined with both Fam91a1 and WDR11 stability.

In addition, we used the Qiagen's data-mining Ingenuity Pathway Analysis® (IPA) software to analyze the proteomics data which confirmed autophagy as major canonical pathway changed in the absence of Fam91a1, as well as Sertoli cell signaling (Fig. 11f). The literature reported an interesting connection between retrograde transport machinery, specifically Golgi-to-ER, and autophagy regulation and function (autophagy regulators trafficking)<sup>75</sup>. In particular, Beclin-1 (BECN1), Autophagy related 9A (ATG9A) and Vacuolar protein sorting 18 (Vps18) were discovered to be significantly downregulated in Fam91a1 knock-down HeLa cells. Beclin-1 is a key factor of autophagy which also plays different influential roles in retrograde trafficking, phagosome maturation<sup>93,94</sup> and endocytosis<sup>95</sup>. ATG9a, a multipass transmembrane ATG protein<sup>96</sup> that cooperates in the formation and organization of autophagosomes and phagophore assembly<sup>75</sup> by a poorly described mechanism that involves cycling of ATG9a-containing vesicles between the trans-Golgi network (TGN), plasma membrane, recycling endosomes and autophagic membranes<sup>96,97</sup>. Vps18, plays a role in vesicle-mediated protein trafficking to lysosomal compartments, as a part of the endo-lysosomal system. In particular, part of the complexes HOPS and CORVET that coordinate tethering and fusion events in endosomes and lysosomes. Both of these complexes are implicated in

the regulation of autophagic trafficking towards lysosomes<sup>98,99</sup>. WASH6, another protein downregulated in Fam91a1 knock-down, is a WASH family protein. The WASH complex is an endosome sorting hub important in recycling and trafficking of membrane proteins, including  $\alpha 5\beta 1$  integrin<sup>100</sup>.

Altogether, literature illustrates a potential association between the aforementioned proteins; for example, Vps35 (retromer complex subunit) mutations impair WASH complex recruitment to endosomes which leads to inhibition of autophagy, due to deficient trafficking of ATG9a, and result in a role of WASH complex in autophagosome formation<sup>101</sup>. Allied with a study showing that Vps13 depletion (one of the proteins already mentioned to be commonly downregulated in Fam91a1 and WDR11) was associated with an accumulation of autophagy markers and impaired autophagy flux<sup>60</sup>. Also, a Beclin-1-binding autophagic factor (UVRAG), along with the vesicle fusion complex (SNARE), mediate ER tethering and fusion events. When these UVRAG-mediated tethering and fusion events are impaired, it affects Golgi-to-ER retrograde trafficking, disrupting Golgi structure<sup>75</sup>. Such disruption was reported to hinder the exit of ATG9-positive vesicles from the Golgi, thus blocking membrane expansion from autophagosomes<sup>75</sup>.

Moreover, induction of autophagy can require the activation of PIK3C3/Vps34 within a multiprotein complex that contains Beclin-1. When depleted of Beclin-1, cells cannot form phagophores and autophagosomes because of the inhibition of a cis-unsaturated fatty acid producing enzyme<sup>102</sup>. Another study reported the high dependency of the functional TGN membranes for the correct autophagosome formation, in a mechanism mediated by Beclin-1/Vps34 complex and proper ATG9 trafficking<sup>103</sup>.

Besides autophagy, Sertoli cell signaling (Sertoli cells assist the process of spermatogenesis) was another pathway identified by proteomics to be affected in the Fam91a1 knock-down. Spectrin beta 1 (SPB1), Y-Box binding protein 3 (YXB3), Plastin 1 (PLS1) and the small GTPase Rab 8 (Rab8b), as well as PLIN2 (downregulated in shWDR11), are worth mentioning in this context due to the tight link between *WDR11* gene mutations and idiopathic hypogonadotropic hypogonadism (IHH) and Kallmann's

syndrome (KS), both related to deficient pubertal development caused by low levels of sex steroid production<sup>67</sup>.

Although not yet fully analyzed and interpreted, the initial reviewing of the interactomes of WDR11- and C17orf75-BioID biotin pull down partially showed concordant results with the whole-proteome screening and thorough analysis of the proteins downregulated in Fam91a1 knock-down. Surprisingly, C17orf75-BioID interactome was the one which showed most similar classes of protein interactors, compared to the ones found downregulated in Fam91a1 knock-down, like ATG9 and Perilipin 4. It is also important to notice that Cl-M6Pr and Talin, a major binding interactor of integrins, were also biotinylated and pulled-down in C17orf75-BioID cells. Regarding WDR11-BioID biotinylated pull-down interactome, the most apparently interesting proteins captured were mostly Vps complex subunits, like Vps 51, Vps52 and Vps53 (GARP subunits), suggesting a possible connection between the GARP complex and the Fam91a1/WDR11/C17orf75 complex, Vps33a and Vps45.

In summary, this mass-spectrometry screening both of whole-proteome or interactome proteins, revealed a remarkable association between the Fam91a1/WDR11/C17orf75 complex and autophagy, endocytic signaling and pubertal development. Further studies will be required to establish the link between proteins downregulated in Fam91a1 knock-down and the discovered pathways.

# Concluding Remarks





## Concluding Remarks

Up to now retrograde transport was a largely unexplored intracellular route for integrin trafficking. In the present study we identified a trimeric complex composed of Fam91a1, WDR11 and C17orf75 that plays a role in TGN-mediated retrograde trafficking and localization of  $\beta$ 1 integrins.

Previous proteomic screenings identified candidate cytoplasmic  $\alpha$ 5 $\beta$ 1 integrin interactors which localize to intracellular organelles involved in retrograde trafficking. By co-immunoprecipitation and biotinylation experiments we were able to characterize a Golgi-localized complex composed of Fam91a1, WDR11 and C17orf75, whose stability is Fam91a1-dependent confirming previously reported interactions between some of the proteins. Depletion of members of this complex in HeLa cells resulted in impaired trafficking of known TGN cargos, CI-M6Pr and TGN46, and increased localization to dispersed vesicles, similar to retromer and GARP complexes depleted cells.

A recent study discovered that  $\alpha$ 5 $\beta$ 1 integrin traffics via a retrograde transport and we also observed altered  $\alpha$ 5 $\beta$ 1 integrin subcellular localization upon depletion of the Fam91a1/WDR11/C17orf75 complex. As  $\alpha$ 5 $\beta$ 1 integrins were misrouted from focal adhesions, wound healing assays showed that cell migration speed and randomness were reduced.

Proteomic screenings suggested that Fam91a1/WDR11/C17orf75 complex might be essentially associated with other processes such as autophagy, endocytic signaling and pubertal development.

Nevertheless, future research on this trimeric complex and overall retrograde trafficking of integrins is important to fully understand how integrin availability at the cell surface is regulated which has a direct effect on integrin function and the integrin-mediated cellular processes.



# Materials & Methods



## 1. Antibodies

The following antibodies were used for western blotting (WB) and immunofluorescence (IF): actin (A-2066, Sigma; 1:3000 for WB),  $\alpha 5$  integrin (4705, Cell Signaling; for IF),  $\alpha$ -tubulin (2144, Cell Signaling; 1:5000 for WB),  $\beta 1$  integrin (Chemicon; 1:400 for IF), C17orf75 (SAB1405246, Sigma; 1:400 for WB), CI-M6Pr (ABCam; 1:250 [live incubation] 1:500 [fixed incubation] for IF), Fam91a1 (PA5-24948, Thermo, Sta. Cruz; 1:400 for WB; 1:1000 for IF), GFP (A11122, Invitrogen; 1:1000 for WB; 1:1500 for IF), GM130 (610822, BD; 1:1000 for IF) HA-tag (H6908, Sigma; for IF), Paxilin (ab32084, ABCam; 1:300 for IF), Phalloidin (A12379, Alexa488, Molecular Probes; 1:600 for IF), Streptavidin (016-160-084, cy3, Jackson; 1:300 for IF), Syndetin (FLJ20097, ABnova; for WB and IF), TGN46 (AHP500G, AbD Serotec; 1:1500 for WB and IF), WDR11 (AB93871, ABCam; 1:1000 for WB and IF). DAPI (Sigma) was used to stain nuclei.

## 2. Constructs and Transfections

All the constructs and respective stable transfections/cell lines of HeLa cells or fibroblasts used in this study were designed, produced and performed by Dr. Ralph Thomas Böttcher: Silencing small-hairpin RNAs shFam91a1 #6/#8, shC17orf75, shWDR11. HA-tagged Biotin ligase constructs for BioID experiments<sup>1</sup> C17orf75-BioID-HA and  $\alpha 5$ -BioID-HA. Point mutations of GFP-tagged WDR11 (A435T, H690Q, HH507/513AA). shRNA-resistant GFP-tagged Fam91a1. Constructs of siVps53, siVps54 and siSyndetin were bought from GE Healthcare.

Cells were transiently transfected with Lipofectamine 2000 (Invitrogen) in Opti-MEM medium for 6 hours, according to the manufacturer's protocol.

## 3. Cell Culture

The cell lines used in this study are immortalized cervical cancer standard HeLa cells stably expressing shFam91a1, shC17orf75 or shWDR11 knock-downs. Or  $\beta 1$  flox fibroblasts transiently expressing siVps53, siVps54 or siSyndetin. All cells cultured were detached with trypsin-EDTA before each passage to a new plate. Were cultured under standard cell culture conditions using Dulbecco's modified Eagle's medium (DMEM; Invitrogen) supplemented with 10% (v/v) fetal bovine serum (FBS) and, unless stated

otherwise, 1% Penicillin/Streptomycin (P/S; Invitrogen) at 37°C and 5% CO<sub>2</sub>. Cells were not subjected to mycoplasma contamination testing.

#### **4. Cell lysis and Western Blotting**

For cell lysis, 10 cm dishes were collected, washed 3x times with PBS and added with  $\beta$ 1 lysis buffer (modified RIPA buffer) (0.05% (w/v) sodium deoxycholate, 0.1% SDS (w/v), 1% Triton X-100, 50 mM Tris-HCl [pH 8.0], 150 mM NaCl, 10 mM EDTA, ddH<sub>2</sub>O) with protease and phosphatase inhibitors (Roche) for 10 minutes at 4 °C. Lysates were sonicated for 10s and centrifuged at 13,200g for 10 min at 4°C and stored with 4x SDS-loading buffer (1% SDS, 100 mM Tris-HCl pH 6.8, 10% Glycerol, 0.001% Bromophenol Blue, 4%  $\beta$ -mercaptoethanol) at -20°C. Protein quantification was performed according to standard BCA assay.

Supernatants were separated by 8% gel SDS-PAGE. After transfer to polyvinylidene fluoride (PVDF) membrane for 2 hours at 4 °C, membranes were blocked in milk- or 3% BSA-TBS-Tween (0.1%) and incubated at 4°C overnight with primary antibody. Detection was performed by enhanced chemiluminescence after 1-hr incubation with horseradish-peroxidase (HRP)-conjugated secondary antibodies and image acquisition with peroxide/luminal (ECF) solution. Scanning densitometry was performed using the ImageJ software.

#### **5. Immunoprecipitations and Biotin pull-downs**

Selective isolation of Fam91a1 and WDR11, as well as the rest of the trimeric complex components, was achieved by co-immunoprecipitation. Cells were lysed as previously described, and incubated with either rabbit IgG, anti-WDR11 or anti-Fam91a1 antibodies, for 1 hour at 4 °C. G Sepharose (Sigma) beads coated with protein A and G were washed 3x times with 500  $\mu$ l lysis buffer.

The trimeric complex (Fam91a1/WDR11/C17orf75) was pulled down by incubating lysate samples with 50  $\mu$ l of beads incubated for 2 hours at 4 °C subjected to gentle rotation. Beads-protein complexes were washed 3x times with lysis buffer for 2 minutes at 4000 rpms, followed SDS-PAGE and western blot analysis as described.

For the biotinylation assay, HeLa + shC17orf75 + C17orf75-BioID-HA and HeLa  $\alpha$ 5-BioID-HA cell lines were incubated with 100  $\mu$ M of biotin overnight (24 hours). Cell plates were washed 2x times with PBS, incubated for 1 hour 37  $^{\circ}$ C with normal DMEM/FBS/PS medium and then lysed as described before. After determining concentration, a small aliquot was removed for whole cell lysates. 1000  $\mu$ g of lysate were then mixed with lysis buffer + protease inhibitor and 1  $\mu$ l of 1 M DTT. 50  $\mu$ l of 3x times washed Streptavidin-Sepharose beads were added to the lysates and incubated overnight at 4  $^{\circ}$ C rotating. The next day beads were washed 3x times with PBS + 0.5 M NaCl + 1% Triton-X100, then to break beads-protein link, beads were mixed with 80  $\mu$ l of 4x SDS-loading buffer and cooked for 7 min at 95  $^{\circ}$ C. After centrifugation, supernatant was collected and stored at -20  $^{\circ}$ C. Lysates were separated by 8% gel SDS-PAGE and western blot analysis as described before.

## **6. Immunofluorescence Microscopy**

For immunostainings, cells were cultured on glass coated with 10  $\mu$ g ml<sup>-1</sup> fibronectin (Calbiochem). For following Cl-M6Pr trafficking in live cells, Cl-M6Pr (1:300) Cells were fixed with 4% (w/v) PFA/PBS for 15 min at room temperature, washed with pre-warmed PBS (37 $^{\circ}$ C) and permeabilized with either 0.1% Triton X/PBS or 0.01% Saponin/PBS for 10 min at room temperature or ice. Cells were blocked with 3 % BSA/PBS for 1 hour at room temperature followed by incubation with the primary antibody in 3% BSA/PBS overnight at 4 $^{\circ}$ C and secondary antibodies for 1 hour at room temperature in the dark. Coverslips were mounted with Evanol (Mowiol and Dabco, Sigma) and DAPI (Sigma) to counterstain nuclei.

Fluorescent images were acquired with a AxioVision Apotome fluorescence microscopy (Carl Zeiss, Germany) equipped with 63x/oil objective, using multidimension acquisition feature. Contrast adjustment, editing and further image analysis were performed in ImageJ (v1.47) and Adobe Illustrator software.

## **7. Cycloheximide chase assay**

1x10<sup>6</sup> HeLa cells stably expressing shFam91a1 and shWDR11 were seeded on 10 cm dishes with full DMEM medium, after attachment to the base of the plate medium was



changed to starving 0.2% FBS DMEM/PS and incubated overnight. Dishes were washed with PBS and incubated with 20  $\mu\text{g/ml}$  of Cycloheximide, to inhibit protein synthesis, in the same starving medium conditions at 37  $^{\circ}\text{C}$  and TGN46 chased for the different time-points (0, 3 and 8 hours) followed lysis and storage of lysates at  $-20^{\circ}\text{C}$ . Lysates were separated by 8% gel SDS-PAGE and western blot analysis as described before.

## **8. Scratch wound healing assays**

Scratch wound healing assays were performed with 6-well dishes coated with 10  $\mu\text{g ml}^{-1}$  fibronectin (Calbiochem) and confluent monolayers of cells-serum starved overnight at 37  $^{\circ}\text{C}$ . Afterwards, to limit cell proliferation cells were treated with Mitomycin C (Sigma, 25  $\mu\text{g ml}^{-1}$ ) for 2 hours in serum-free Penicillin/Streptomycin-free DMEM medium at 37  $^{\circ}\text{C}$  before wounds were applied with a 200  $\mu\text{l}$  plastic micropipette followed by thorough washing with PBS and imaging.

## **9. Live-cell imaging by time-lapse video microscopy**

Wound closure was imaged in serum-free DMEM medium at 20 minute intervals overnight (24 hours). Images of live cells were recorded at 37  $^{\circ}\text{C}$  and 5%  $\text{CO}_2$  on a Zeiss Axiovert 200M (Carl Zeiss, Germany) equipped with x10/.3 x16/.3 and x20/.4 objectives, a motorized stage (Märzhäuser, Germany) and an environment chamber (EMBL Precision Engineering) with a cooled CCD (charged-coupled device) camera (Roper Scientific, Princeton, NJ). Image acquisition and microscope control were carried out with MetaMorph software (Molecular Devices).

From time-lapse videos, a total of approximately 50 migrating cells per condition (shCtr, shFam91a1 #6/#8, shWDR11, shFam91a1 #6 + GFP-Fam91a1) from 3 independent experiments were analyzed using the manual tracking plugin of ImageJ and the Chemotaxis and Migration Tool (v2.0) of the QWT project.

## **10. Mass Spectrometry and Analysis**

For whole-proteome mass spectrometry (MS) screening of Hela shCtr, shFam91a1, shWDR11, 3x 10 cm dishes of each condition were collected, thoroughly washed 5x times with PBS and lysed with 100  $\mu\text{l}$  of MS-buffer (6 M GnHCl, 10 mM TCEP, 40 mM 2-

Chloroacetamide), spin-down and supernatants were taken to *in-house* core facility for MS screening. The proximity biotinylation interactome MS screening of HeLa + shC17orf75 + C17orf75-BioID-HA and HeLa + shWDR11 + WDR11-BioID-HA was performed by Dr. Ralph Thomas Böttcher.

To analyze the results from both whole-proteome and interactome MS screenings, a Perseus software (v1.5.2.11) adjusted analysis protocol was used. Briefly, 'ProteinGroups.txt' files containing the raw results from the MS screenings were loaded into the software, and 8159 hits were registered for the whole-proteome screening of Fam91a1 and WDR11 knock-downs, 790 for the WDR-BioID and 615 for C17orf75-BioID.

Analysis was based on the different LFQ intensities registered for each protein compared to the control. Protein hits without LFQ intensity values on the 3 replicates on at least one condition were discarded and missing values were replaced by a normal distribution. 1-way ANOVA ( $S_0 = 0.5$ , Permutation-based FDR = 0.05) statistical test and Z-Score transformation were applied. Final filtered results were displayed using Hierarchical clustering and Profile plots. Special thanks to Dr. Nagarjuna Nagaraj (head of Mass-Spec and Proteomics MPI of Biochemistry Core facility) for the insights and help on developing the protocol.

Qiagen Ingenuity Pathway Analysis® (IPA) data mining software analysis of the most statistically significant downregulated protein expression of Fam91a1 KD in categorical groups of Canonical Pathways and Networks was kindly provided by Scientific Information Services of the MPI of Biochemistry.

## **11. Statistical Analysis**

Statistical analysis was performed using the GraphPad Prism software (version 5.00, GraphPad Software). Statistical significance was determined by 1-way ANOVA test. Results are expressed as means  $\pm$  standard error of mean (S.E.M.). Values were considered significant at P (P-value) < 0.05.



# Bibliography



1. Hynes, R. O. Integrins : Bidirectional , Allosteric Signaling Machines In their roles as major adhesion receptors , integrins. *Cell* **110**, 673–687 (2002).
2. Barczyk, M., Carracedo, S. & Gullberg, D. Integrins. *Cell Tissue Res.* **339**, 269–280 (2010).
3. Humphries, M. J., Symonds, E. J. H. & Mould, A. P. Mapping functional residues onto integrin crystal structures. *Curr. Opin. Struct. Biol.* **13**, 236–243 (2003).
4. Legate, K. R., Wickström, S. a, Fässler, R., Fa, R. & Wickstro, S. a. Genetic and cell biological analysis of integrin outside-in signaling Genetic and cell biological analysis of integrin outside-in signaling. 397–418 (2009). doi:10.1101/gad.1758709
5. Zent, R. & Pozzi, A. Cell-extracellular matrix interactions in cancer. *Cell-Extracellular Matrix Interact. Cancer* 1–314 (2010). doi:10.1007/978-1-4419-0814-8
6. Calderwood, D. a *et al.* Integrin beta cytoplasmic domain interactions with phosphotyrosine-binding domains: a structural prototype for diversity in integrin signaling. *Proc. Natl. Acad. Sci. U. S. A.* **100**, 2272–2277 (2003).
7. Luo, B. H. & Springer, T. A. Integrin structures and conformational signaling. *Curr. Opin. Cell Biol.* **18**, 579–586 (2006).
8. Moser, M., Legate, K. R., Zent, R. & Fassler, R. The Tail of Integrins, Talin, and Kindlins. *Science (80-. ).* **324**, 895–899 (2009).
9. Pankov, R. *et al.* Integrin dynamics and matrix assembly: Tensin-dependent translocation of  $\alpha 5 \beta 1$  integrins promotes early fibronectin fibrillogenesis. *J. Cell Biol.* **148**, 1075–1090 (2000).
10. Clark, K. *et al.* A specific  $\alpha 5 \beta 1$ -integrin conformation promotes directional integrin translocation and fibronectin matrix formation. *J. Cell Sci.* **118**, 291–300 (2005).
11. Valdem bri, D. & Serini, G. Regulation of adhesion site dynamics by integrin traffic. *Curr. Opin. Cell Biol.* **24**, 582–591 (2012).

12. Danen, E. H. J., Sonneveld, P., Brakebusch, C., Fässler, R. & Sonnenberg, A. The fibronectin-binding integrins  $\alpha 5\beta 1$  and  $\alpha v\beta 3$  differentially modulate RhoA-GTP loading, organization of cell matrix adhesions, and fibronectin fibrillogenesis. *J. Cell Biol.* **159**, 1071–1086 (2002).
13. Chen, L., Vicente-Manzanares, M., Potvin-Trottier, L., Wiseman, P. W. & Horwitz, A. R. The integrin-ligand interaction regulates adhesion and migration through a molecular clutch. *PLoS One* **7**, (2012).
14. Ponti, A., Machacek, M., Gupton, S. L., Waterman-Storer, C. M. & Danuser, G. Two distinct actin networks drive the protrusion of migrating cells. *Science* **305**, 1782–6 (2004).
15. Parsons, J. T., Horwitz, A. R. & Schwartz, M. a. Cell adhesion: integrating cytoskeletal dynamics and cellular tension. *Nat. Rev. Mol. Cell Biol.* **11**, 633–43 (2010).
16. Pellinen, T. & Ivaska, J. Integrin traffic. *J. Cell Sci.* **119**, 3723–3731 (2006).
17. De Franceschi, N., Hamidi, H., Alanko, J., Sahgal, P. & Ivaska, J. Integrin traffic - the update. *J. Cell Sci.* **128**, 839–52 (2015).
18. Caswell, P. T., Vadrevu, S. & Norman, J. C. Integrins: masters and slaves of endocytic transport. *Nat. Rev. Mol. Cell Biol.* **10**, 843–853 (2009).
19. Chao, W. T. & Kunz, J. Focal adhesion disassembly requires clathrin-dependent endocytosis of integrins. *FEBS Lett.* **583**, 1337–1343 (2009).
20. Shi, F. & Sottile, J. Caveolin-1-dependent beta1 integrin endocytosis is a critical regulator of fibronectin turnover. *J. Cell Sci.* **121**, 2360–71 (2008).
21. Caswell, P. T. & Norman, J. C. Integrin trafficking and the control of cell migration. *Traffic* **7**, 14–21 (2006).
22. Paul, N. R., Jacquemet, G. & Caswell, P. T. Endocytic Trafficking of Integrins in Cell Migration. *Curr. Biol.* **25**, R1092–R1105 (2015).
23. Roberts, M. S., Woods, A. J., Dale, T. C., Van Der Sluijs, P. & Norman, J. C. Protein kinase B/Akt acts via glycogen synthase kinase 3 to regulate recycling of alpha v beta 3 and alpha 5 beta 1 integrins. *Mol. Cell. Biol.* **24**, 1505–1515 (2004).
24. Powelka, A. M. *et al.* Stimulation-Dependent Recycling of Integrin b1 Regulated by ARF6 and Rab11. *Traffic* 1–18 (2004). doi:10.1046/j.1600-0854.2003.00150.x

25. Caswell, P. T. *et al.* Rab-coupling protein coordinates recycling of  $\alpha 5 \beta 1$  integrin and EGFR1 to promote cell migration in 3D microenvironments. *J. Cell Biol.* **183**, 143–155 (2008).
26. Brandizzi, F. & Barlowe, C. Organization of the ER-Golgi interface for membrane traffic control. *Nat. Rev. Mol. Cell Biol.* **14**, 382–92 (2013).
27. Johannes, L. & Popoff, V. Tracing the Retrograde Route in Protein Trafficking. *Cell* **135**, 1175–1187 (2008).
28. Bonifacino, J. S. & Glick, B. S. The Mechanisms of Vesicle Budding and Fusion. *Cell* **116**, 153–166 (2004).
29. Hirata, T. *et al.* Post-Golgi anterograde transport requires GARP-dependent endosome-to-TGN retrograde transport. *Mol. Biol. Cell* **26**, 3071–3084 (2015).
30. Bonifacino, J. S. & Rojas, R. Retrograde transport from endosomes to the trans-Golgi network. *Nat. Rev. Mol. Cell Biol.* **7**, 568–579 (2006).
31. Taylor, K. E. & Mossman, K. L. Cellular Protein WDR11 Interacts with Specific Herpes Simplex Virus Proteins at the trans -Golgi Network To Promote Virus Replication. *J. Virol.* **89**, 9841–9852 (2015).
32. Sandvig, K. & van Deurs, B. Delivery into cells: lessons learned from plant and bacterial toxins. *Gene Ther.* **12**, 865–872 (2005).
33. Bassik, M. C. *et al.* A systematic mammalian genetic interaction map reveals pathways underlying ricin susceptibility. *Cell* **152**, 909–922 (2013).
34. Rojas, R. *et al.* Regulation of retromer recruitment to endosomes by sequential action of Rab5 and Rab7. *J. Cell Biol.* **183**, 513–26 (2008).
35. Bonifacino, J. S. & Traub, L. M. Signals for Sorting of Transmembrane Proteins to Endosomes and Lysosomes\*. *Annu. Rev. Biochem.* **72**, 395–447 (2003).
36. Gruenberg, J. & Stenmark, H. The biogenesis of multivesicular endosomes. *Nat. Rev. Mol. Cell Biol.* **5**, 317–323 (2004).
37. Chia, P. Z. C., Gunn, P. & Gleeson, P. A. Cargo trafficking between endosomes and the trans-Golgi network. *Histochem. Cell Biol.* **140**, 307–315 (2013).
38. Mallard, F. *et al.* Direct pathway from early/recycling endosomes to the Golgi apparatus revealed through the study of shiga toxin B-fragment transport. *J. Cell Biol.* **143**, 973–90 (1998).



39. Liewen, H. *et al.* Characterization of the human GARP (Golgi associated retrograde protein) complex. *Exp. Cell Res.* **306**, 24–34 (2005).
40. Perez-Victoria, F. J., Mardones, G. A. & Bonifacino, J. S. Requirement of the Human GARP Complex for Mannose 6-phosphate-receptor-dependent Sorting of Cathepsin D to Lysosomes. *Mol. Biol. Cell* **19**, 2350–2362 (2008).
41. Hong, W. SNAREs and traffic. *Biochim. Biophys. Acta - Mol. Cell Res.* **1744**, 120–144 (2005).
42. Lombardi, D. *et al.* Rab9 functions in transport between late endosomes and the trans Golgi network. *EMBO J.* **12**, 677–82 (1993).
43. Mckenzie, J. E. *et al.* Retromer Guides STxB and CD8-M6PR from Early to Recycling Endosomes, EHD1 Guides STxB from Recycling Endosome to Golgi. *Traffic* **13**, 1140–1159 (2012).
44. Mallard, F. *et al.* Early/recycling endosomes-to-TGN transport involves two SNARE complexes and a Rab6 isoform. *J. Cell Biol.* **156**, 653–664 (2002).
45. Schindler, C., Chen, Y., Pu, J., Guo, X. & Bonifacino, J. S. EARP is a multisubunit tethering complex involved in endocytic recycling. *Nat. Cell Biol.* **17**, 639–650 (2015).
46. Hong, W. & Lev, S. Tethering the assembly of SNARE complexes. *Trends Cell Biol.* **24**, 35–43 (2014).
47. Spang, A. Membrane Tethering Complexes in the Endosomal System. *Front. Cell Dev. Biol.* **4**, 1–7 (2016).
48. Arjonen, A., Alanko, J., Veltel, S. & Ivaska, J. Distinct Recycling of Active and Inactive  $\beta$ 1 Integrins. *Traffic* **13**, 610–625 (2012).
49. Shafaq-Zadah, M. *et al.* Persistent cell migration and adhesion rely on retrograde transport of  $\beta$ 1 integrin. *Nat. Cell Biol.* **18**, 54–64 (2016).
50. Bonifacino, J. S. & Hurley, J. H. Retromer. *Curr. Opin. Cell Biol.* **20**, 427–436 (2008).
51. Seaman, M. N. J. The retromer complex - endosomal protein recycling and beyond. *J. Cell Sci.* **125**, 4693–702 (2012).
52. Zerial, M. & McBride, H. Rab proteins as membrane organizers. *Nat. Rev. Mol. Cell Biol.* **2**, 107–117 (2001).

53. Conibear, E., Cleck, J. N. & Stevens, T. H. Vps51p mediates the association of the GARP (Vps52/53/54) complex with the late Golgi t-SNARE Tlg1p. *Mol. Biol. Cell* **14**, 1610–23 (2003).
54. Bonifacino, J. S. & Hierro, A. Transport according to GARP: Receiving retrograde cargo at the trans-Golgi network. *Trends Cell Biol.* **21**, 159–167 (2011).
55. Cullen, P. J. Endosomal sorting and signalling: an emerging role for sorting nexins. *Nat. Rev. Mol. Cell Biol.* **9**, 574–82 (2008).
56. Cullen, P. J. & Korswagen, H. C. Sorting nexins provide diversity for retromer-dependent trafficking events. *Nat. Cell Biol.* **14**, 29–37 (2012).
57. Böttcher, R. T. *et al.* Sorting nexin 17 prevents lysosomal degradation of  $\beta$ 1 integrins by binding to the  $\beta$ 1-integrin tail. *Nat. Cell Biol.* **14**, 584–92 (2012).
58. Tseng, H. Y. *et al.* Sorting nexin 31 binds multiple  $\beta$  integrin cytoplasmic domains and regulates  $\beta$ 1 integrin surface levels and stability. *J. Mol. Biol.* **426**, 3180–3194 (2014).
59. Lum, J. J., DeBerardinis, R. J. & Thompson, C. B. Autophagy in metazoans: cell survival in the land of plenty. *Nat. Rev. Mol. Cell Biol.* **6**, 439–48 (2005).
60. Muñoz-Braceras, S., Calvo, R. & Escalante, R. TipC and the chorea-acanthocytosis protein VPS13A regulate autophagy in Dictyostelium and human HeLa cells. *Autophagy* **11**, 918–927 (2015).
61. Behrends, C., Sowa, M. E., Gygi, S. P. & Harper, J. W. Network organization of the human autophagy system. *Nature* **466**, 68–76 (2010).
62. Tuloup-Minguez, V. *et al.* Autophagy modulates cell migration and  $\beta$ 1 integrin membrane recycling. *Cell Cycle* **12**, 3317–3328 (2013).
63. Sharifi, M. N. *et al.* Autophagy Promotes Focal Adhesion Disassembly and Cell Motility of Metastatic Tumor Cells through the Direct Interaction of Paxillin with LC3. *Cell Rep.* **15**, 1660–1672 (2016).
64. Han, M. H. J. *et al.* Dysbindin-associated proteome in the P2 synaptosome fraction of mouse brain. *J. Proteome Res.* **13**, 4567–4580 (2014).
65. Nakamura, N. *et al.* Characterization of a. **131**, 1715–1726 (1995).

66. Roux, K. J., Kim, D. I., Raida, M. & Burke, B. A promiscuous biotin ligase fusion protein identifies proximal and interacting proteins in mammalian cells. *J. Cell Biol.* **196**, 801–810 (2012).
67. Kim, H. G. *et al.* WDR11, a WD protein that interacts with transcription factor EMX1, is mutated in idiopathic hypogonadotropic hypogonadism and Kallmann syndrome. *Am. J. Hum. Genet.* **87**, 465–479 (2010).
68. Klinger, S. C., Siupka, P. & Nielsen, M. S. Retromer-mediated trafficking of transmembrane receptors and transporters. *Membranes (Basel)*. **5**, 288–306 (2015).
69. Arighi, C. N., Harmell, L. M., Aguilar, R. C., Haft, C. R. & Bonifacino, J. S. Role of the mammalian retromer in sorting of the cation-independent mannose 6-phosphate receptor. *J. Cell Biol.* **165**, 123–133 (2004).
70. Seaman, M. N. J. Cargo-selective endosomal sorting for retrieval to the Golgi requires retromer. *J. Cell Biol.* **165**, 111–122 (2004).
71. Wang, S. *et al.* A role of Rab29 in the integrity of the trans-golgi network and retrograde trafficking of mannose-6-phosphate receptor. *PLoS One* **9**, 1–12 (2014).
72. Pérez-Victoria, F. J. & Bonifacino, J. S. Dual roles of the mammalian GARP complex in tethering and SNARE complex assembly at the trans-golgi network. *Mol. Cell Biol.* **29**, 5251–63 (2009).
73. Conibear, E. & Stevens, T. H. Vps52p, Vps53p, and Vps54p form a novel multisubunit complex required for protein sorting at the yeast late Golgi. *Mol. Biol. Cell* **11**, 305–323 (2000).
74. Aveland, M. I. & Oresti, G. M. Cell-type-specific regulation of genes involved in testicular lipid metabolism: fatty acid-binding proteins, diacylglycerol acyltransferases, and perilipin 2'. (2010). doi:10.1530/REP-13-0199
75. He, S. *et al.* PtdIns(3)P-bound UVRAG coordinates Golgi-ER retrograde and Atg9 transport by differential interactions with the ER tether and the beclin 1 complex. *Nat. Cell Biol.* **15**, 1206–19 (2013).
76. Smith, T. F., Gaitatzes, C., Saxena, K. & Neer, E. J. The WD repeat: A common architecture for diverse functions. *Trends Biochem. Sci.* **24**, 181–185 (1999).

77. Izumi, Y., Suzuki, E., Kanzaki, S., Yatsuga, S. & Kinjo, S. Genome-wide copy number analysis and systematic mutation screening in 58 patients with hypogonadotropic hypogonadism. *FNS* **102**, 1130–1136.e3 (2014).
78. Weidberg, H. *et al.* LC3 and GATE-16 / GABARAP subfamilies are both essential yet act differently in autophagosome biogenesis. *EMBO J.* **29**, 1792–1802 (2010).
79. Nakamura, T. *et al.* PX-RICS mediates ER-to-Golgi transport of the N-cadherin /  $\beta$ -catenin complex. 1244–1256 (2008). doi:10.1101/gad.1632308.mic
80. Hayashi-nishino, M., Fujita, N., Noda, T., Yamaguchi, A. & Yoshimori, T. A subdomain of the endoplasmic reticulum forms a cradle for autophagosome formation. *Nat. Cell Biol.* **11**, 1433–1437 (2009).
81. Ylä-anttila, P., Vihinen, H., Jokitalo, E. & Eskelinen, E. phagophore and endoplasmic reticulum 3D tomography reveals connections between the phagophore and endoplasmic reticulum. **8627**, (2016).
82. Griffiths, G. & Simons, K. A. I. trans Golgi Network : Sorting at the Exit Site of the Golgi Complex The TGN-the Exit Compartment of the.
83. Gadila, S. K. G. & Kim, K. Cargo trafficking from the trans-Golgi network towards the endosome. *Biol. Cell* **108**, 1–14 (2016).
84. Liu, J. J. Retromer-Mediated Protein Sorting and Vesicular Trafficking. *J. Genet. Genomics* **43**, 165–177 (2015).
85. Wan, L. *et al.* PACS-1 Defines a Novel Gene Family of Cytosolic Sorting Proteins Required for trans -Golgi Network Localization. **94**, 205–216 (1998).
86. Nonnenmacher, M. E., Cintrat, J.-C., Gillet, D. & Weber, T. Syntaxin 5-dependent retrograde transport to the trans-Golgi network is required for adeno-associated virus transduction. *J. Virol.* **89**, 1673–1687 (2015).
87. Topalidou, I. *et al.* The EARP Complex and Its Interactor EIPR-1 Are Required for Cargo Sorting to Dense-Core Vesicles. *PLOS Genet.* **12**, e1006074 (2016).
88. Rossier, O. *et al.* Integrins  $\beta$ 1 and  $\beta$ 3 exhibit distinct dynamic nanoscale organizations inside focal adhesions. *Nat. Cell Biol.* **14**, 1057–1067 (2012).
89. White, D. P., Caswell, P. T. & Norman, J. C.  $\beta$ 3 and  $\beta$ 1 integrin recycling pathways dictate downstream Rho kinase signaling to regulate persistent cell migration. *J. Cell Biol.* **177**, 515–525 (2007).

90. Huang, S. *et al.* A new microRNA signal pathway regulated by long noncoding RNA TGFB2-OT1 in autophagy and inflammation of vascular endothelial cells. *Autophagy* **8627**, 2172–2183 (2015).
91. Ordoñez, Y. F. *et al.* 3-Ketosphinganine provokes the accumulation of dihydroshingolipids and induces autophagy in cancer cells. *Mol. BioSyst.* **12**, 1166–1173 (2016).
92. Moreau, K. & Rubinsztein, D. C. The plasma membrane as a control center for autophagy. *Autophagy* **8**, 861–863 (2012).
93. Liang, X. H. *et al.* Induction of autophagy and inhibition of tumorigenesis by beclin 1. *Nature* **402**, 672–676 (1999).
94. Matsunaga, K. *et al.* Two Beclin 1-binding proteins, Atg14L and Rubicon, reciprocally regulate autophagy at different stages. *Nat. Cell Biol.* **11**, 385–396 (2009).
95. McKnight, N. C. *et al.* Beclin 1 Is Required for Neuron Viability and Regulates Endosome Pathways via the UVRAG-VPS34 Complex. *PLoS Genet.* **10**, 1–18 (2014).
96. Corcelle-Termeau, E. *et al.* Excess sphingomyelin disturbs ATG9A trafficking and autophagosome closure. *Autophagy* **8627**, 1–17 (2016).
97. Puri, C., Renna, M., Bento, C. F., Moreau, K. & Rubinsztein, D. C. ATG16L1 meets ATG9 in recycling endosomes additional roles for the plasma membrane and endocytosis in autophagosome biogenesis. *Autophagy* **10**, 182–184 (2014).
98. Toh, W. H. & Gleeson, P. A. Emerging Insights into the Roles of Membrane Tethers from Analysis of Whole Organisms : The Tip of an Iceberg ? **4**, (2016).
99. Wartosch, L., Gunesdogan, U., Graham, S. C. & Luzio, J. P. Recruitment of VPS33A to HOPS by VPS16 Is Required for Lysosome Fusion with Endosomes and Autophagosomes. *Traffic* 727–742 (2015). doi:10.1111/tra.12283
100. Zech, T. *et al.* The Arp2/3 activator WASH regulates  $\alpha 5\beta 1$ -integrin-mediated invasive migration. *J. Cell Sci.* **124**, 1–7 (2011).
101. Zavodszky, E. *et al.* Mutation in VPS35 associated with Parkinson’s disease impairs WASH complex association and inhibits autophagy. *Nat. Commun.* **5**, 3828 (2014).

102. Niso-Santano, M. *et al.* Novel inducers of BECN1-independent autophagy: Cis-unsaturated fatty acids. *Autophagy* **11**, 575–577 (2015).
103. Guo, Y. *et al.* AP1 is essential for generation of autophagosomes from the trans-Golgi network. *J. Cell Sci.* **125**, 1706–15 (2012).